To the Graduate Council:

I am submitting herewith a thesis written by Junyu Li entitled "Three-Dimensional Rigid Body Trailer Liftoff Model". I have examined the final copy of this thesis for form and content and recommend that it be accepted in partial fulfillment of the requirements for the degree of Master of Science, with a major in Mechanical Engineering.

J. A. M. Boulet, Major Professor

We have read this thesis
and recommend its acceptance:

William R. Hamel

Joe Iannelli

Accepted for the Council:

Interim Vice Provost and
Dean of the Graduate School

Three-Dimensional Rigid Body Trailer Liftoff Model

A Thesis
Presented for the
Master of Science Degree
The University of Tennessee, Knoxville

Junyu Li
August 2001

Acknowledgment

I would like to express my sincere gratitude to Dr. J. A. M. Boulet for his insightful guidance, constant support and invaluable help during the two years I have spent at the University of Tennessee. If it were not Dr. Boulet's advice, encouragement, and patience, so much progress in study and research would not have been possible. I also wish to thank Dr. Hamel and Dr. Iannelli for serving on my advisory committee.

I would also like to extend my sincere appreciation to my father, Gui San Li; my mother, Yu Jin Xiao; my baby brother Guo Yu Li and my sister-in-law Xiao Yan Ju for their love and encouragement. Finally I want to express my appreciation to my husband, Deshun Zhang, for all his love, contribution and support through the years toward my studies and especially toward the completion of my thesis.

Abstract

In this thesis, a new three-dimensional rigid body model for liftoff of the wheels of a heavy commercial truck trailer in steady, circular turning is investigated. For a turn of specified radius, the model predicts two liftoff properties: the speed and roll angle at which liftoff would occur.

Work in this thesis can be divided into two parts. (1) Truck trailer liftoff equations are derived, shown to be internally consistent and used to investigate the importance of several parameters that affect the liftoff properties and roll stability of trailers. Present efforts focus on the modeling of a trailer in a steady maneuver. (2) The model is used on a trailer with one cargo hung from the ceiling of the cargo box. Many factors that influence the liftoff and roll stability of the trailer are discussed. The influence of these parameters on the angular displacement of the cargo itself is also discussed.

The study finds that the influence of trailer weight, path radius, trailer track width, trailer roll stiffness, center of gravity height and lateral location on the liftoff properties and roll stability (resistance to rollover) is high. Also, the influence of roll center height and fore-aft center of gravity location are moderate while the influence of the fifth-wheel height is low. If a change in the system increases either the speed at liftoff or the roll angle of the cargo box at liftoff, we consider that the liftoff properties and roll stability have been improved. The study shows that roll stability and liftoff properties are improved by increasing path radius, trailer track width, roll center height, fifth-wheel height, trailer suspension roll stiffness, or center of gravity longitudinal

distance from the fifth-wheel, and by decreasing the center of gravity height or lateral center of gravity offset.

The model can be used to determine the angular displacement of moving cargos in the cargo box and their influence on the liftoff properties and roll stability of the trailer. A simple example of the usage of the model is given in this thesis. When there is one cargo suspended from the ceiling of the cargo box, increasing path radius or longitudinal distance from the fifth-wheel to the suspension point of the cargo, and decreasing the cargo box height or lateral position of the cargo's suspension point can all improve the liftoff properties and roll stability of the trailer. The model also predicts angular displacement of the hanging cargo.

Table of Contents

List of Figures

Nomenclature

O	path center of the undercarriage center of gravity
A	fifth wheel center
B	contact line of the outer wheel with the ground
P	point where the cargo box and the undercarriage are joined, cargo box rolling center
S	point on the cargo box where a cargo is hung
C	center of gravity of the empty cargo box or cargo box with the fixed cargo inside
Q	center of gravity of the undercarriage
E	center of gravity of the hanging cargo
ψ	roll angle of the cargo box
δ	angle between roll axis of cargo box $\overline{PA}$ and vertical axis
γ	half of the angle composed by the fifth wheel, the path center, and the cargo box
ϕ	elevation angle of the hung cargo from the $(\overline{v}_1, \overline{v}_2)$ plane
θ	azimuthal angle of the hung cargo from axis $\overline{v}_1$
$\Sigma\overline{M}_A$	moment summation about the fifth wheel
$\Sigma\overline{M}_B$	moment summation about outer wheel contact line
$\Sigma\overline{M}_E$	moment summation about the hanging cargo center of gravity
$\overline{M}_P$	interactive moment at P (exerted by cargo box and undercarriage on each other)
$\overline{F}_P$	interactive force at P (exerted by cargo box and undercarriage on each other)

$\overline{F}_S$ interactive force between the hung cargo and cargo box at point S

$\Sigma\overline{F}_E$ force summation about the hanging cargo center of gravity

$\overline{W}_C$ weight of the cargo box

$\overline{W}_U$ weight of the undercarriage

$\overline{W}_E$ hanging cargo weight

$\vec{r}_{12}$ position vector from point 1 to point 2 after the roll of cargo box

$\vec{r}_{12}^{\,o}$ position vector from point 1 to point 2 before the cargo box rolls

m_C mass of the cargo box

m_U mass of the undercarriage

m_E mass of the hanging cargo

$\overline{a}_C$ acceleration of the cargo box at center of gravity C

$\overline{a}_Q$ acceleration of the undercarriage at center of gravity Q

$\overline{a}_E$ acceleration of the hanging cargo at center of gravity E

$\overline{a}_S$ acceleration of the cargo box at point S

$\overline{a}_A$ acceleration of the cargo box at A

$\overline{a}_{1/2}$ acceleration of point *1* relative to the acceleration of point *2*

$\overline{H}_C$ angular momentum of the cargo box at center of gravity C

$\overline{H}_Q$ angular momentum of the undercarriage at center of gravity Q

$\overline{H}_E$ angular momentum of the hanging cargo at center of gravity E

I_C inertia matrix of the cargo box at center of gravity C after the roll

I_C^o inertia matrix of the cargo box expressed in body-axis system

I_Q inertia matrix of the cargo box at center of gravity Q

I_E inertia matrix of the hung cargo at center of gravity E

$\overline{\omega}$ angular velocity of the undercarriage

$\overline{\omega}_C$ angular velocity of the cargo box

$\overline{\omega}_E$ angular velocity of the hanging cargo

$\overline{\Omega}$ relative angular velocity between the cargo box and the undercarriage

$\overline{\Omega}_{E/C}$ relative angular velocity between the cargo box and the hung cargo

$\overline{\alpha}$ angular acceleration of the undercarriage

$\overline{\alpha}_C$ angular acceleration of the cargo box

$\overline{\alpha}_E$ angular acceleration of the hanging cargo

R radius of the horizontal, circular steering path

$\overline{g}$ acceleration of gravity

$\overline{k}, k_0$ roll stiffness of trailer axle suspension

$(\overline{e}_t, \overline{e}_n, \overline{e}_b)$ coordinate system fixed on the undercarriage and originating at point Q

$\overline{e}_t$ unit vector tangent to the path

$\overline{e}_n$ unit vector perpendicular to $\vec{e}_t$ in the horizontal plane and directed to the path center

$\overline{e}_b$ unit vector directed vertically up

$(\overline{U}_1, \overline{U}_2, \overline{U}_3)$ coordinate system originating at point P and fixed relative to undercarriage

$\overline{U}_1$ unit vector directed to the front of the cargo box

$\overline{U}_2$ unit vector that directed to the left of the cargo box

$\overline{U}_3$ unit vector directed vertically up

$(\overline{u}_1, \overline{u}_2, \overline{u}_3)$ coordinate system fixed on the cargo box and originated at point *P*

$\overline{u}_1$ unit vector directed to the front of the cargo box

$\overline{u}_2$ unit vector directed to the left of the cargo box

$\overline{u}_3$ unit vector directed vertically up

$(\overline{v}_1, \overline{v}_2, \overline{v}_3)$ coordinate system fixed on the hanging cargo and originating at point *S*

$\overline{v}_1$ unit vector directed to the rear of the cargo box

$\overline{v}_2$ unit vector directed to the left of the cargo box

$\overline{v}_3$ unit vector directed vertically down

v linear speed of the undercarriage

$\overline{\beta}$ vector defined as $\begin{Bmatrix} \dfrac{d\vec{e}_n}{d\vec{s}} \cdot \vec{e}_b \\ \dfrac{d\vec{e}_b}{d\vec{s}} \cdot \vec{e}_t \\ \dfrac{d\vec{e}_t}{d\vec{s}} \cdot \vec{e}_n \end{Bmatrix}$ in $\{\vec{e}_t, \vec{e}_n, \vec{e}_b\}$ system, which is the reciprocal of the three-dimensional path radius or torsion

τ torsion

ρ radius of path curvature

$R_j(\lambda)$ transformation matrix for rotation around axis *j* through angle λ

R_{1-2} transformation matrix for rotation from coordinate system 1 to 2

L distance between fifth wheel center and the rear roll center

a	longitudinal center of gravity position of empty cargo box
T	trailer axle track width
t	lateral position of the cargo box center of gravity
h	cargo box center of gravity height over fifth-wheel
d	height of fifth-wheel over roll center
p	height of roll center over undercarriage center of gravity
q	roll center height above ground
b	hanging cargo longitudinal position from fifth-wheel
f	hanging cargo lateral position
H	height of cargo box
l	length from cargo suspension point to hanging cargo center of gravity

Chapter 1

Introduction and Problem Description

Rollover accidents of heavy commercial vehicles are of special concern for safety because rollover accidents are especially violent and cause greater damage and injury than other accidents (NASS and GES manual, 1998; Truck and Bus Fact Book, 1995). So, the study of the fundamental mechanics of wheel liftoff and rollover of heavy commercial vehicles is very important in understanding the reason for rollover and helping to decrease the frequency of such accidents.

1.1 The Rollover Process

Rollover is an obvious indicator of vehicle instability. In most literature, trailers are considered as unit vehicles. Most past research has been based on this unit vehicle model. The rollover process in the turn maneuver can be divided into three consecutive phases (Winkler, Blower, Ervin, 1999).

First, the inner spring and tire of the trailer begin to extend and the center of gravity of the cargo box begins to move to outward and to a higher position until at least one tire of the trailer lifts off the ground. This is the liftoff process that precedes every trailer rollover that is not "tripped." (A tripped rollover is initiated by contact of the tire with some object higher than the road, such as a curb.)

The trailer suspension exhibits the highest roll stiffness followed by the tractor drive-axle suspension and then the steer-axle suspension. The stiffness of the latter is quite low compared to the other two (Fancher, Ervin, Winkler, Giliespie, 1986; Laird, 1988; Winkler, Karamihas, Bogard, 1992). The loads carried by (and therefore the maximum load-transfer moments of) the drive-axle and trailer axle suspensions are similar and are each considerably more than the load carried on the steer-axle.

In the liftoff process, the trailer suspension transfers load side-to-side most quickly because of its greater roll stiffness, and is first to arrive at the point of tire liftoff. Roll angle ψ_1 at this moment represents the trailer liftoff. When this occurs, the stiffness of the trailer suspension is "lost" and the "total stiffness" (net resistance to roll, including both gravitational, inertial, and elastic loads) of the system declines. However, the total stiffness is still positive, and the system is still stable even with the trailer tires off the ground.

The second phase of the rollover process is the liftoff of the drive axle of the tractors and rollover of the trailer. The center of gravity continues to move outward and to a higher position until the drive-axle tires lift off the ground. This happens because the roll stiffness of the drive-axle is just a little lower than that of the trailer axle and thus is the next one to liftoff. At this point, the drive-axle stiffness is also lost. The remaining positive stiffness of the steer-axle suspension is far less than the negative influence of the overturning moment. As a result, the total system stiffness is negative, and the vehicle is unstable. The tractor-trailer system is now considered rolled over and the roll angle ψ_2 at this moment represents the rollover threshold. But the phase between the trailer axle liftoff and the drive axle liftoff is highly complex. Sometimes the vehicle loses traction and then loses speed after the liftoff and the lifted wheels settle back onto the ground. On other occasions, rollover may happen faster than expected, partly because of the small difference of roll stiffness between trailer axle suspension and drive-axle suspension. A vehicle with a high center of gravity can roll over in a steady turn maneuver at very low lateral acceleration levels (MacAdam, 1982). Other parameters and factors, such as the drive-axle tire properties, tire pressure (Winkler, Blower, Ervin, 1999), the lash of the drive-axle spring and the fifth-wheel (Winkler, Blower, Ervin, 1999), the torsional compliance of the vehicle frame (Miki, 1988; Winkler, Blower, Ervin, 1999), the lateral compliance of the drive-axle suspension (Fancher, Ervin, Winkler, Giliespie, 1986; Laird, 1988; Winkler, Blower, Ervin, 1999) can all affect this process. Because so many variables are involved, rollover is difficult to predict and can happen quite unexpectedly.

The third phase in the rollover process is what happens after the rollover threshold has been reached—the liftoff of the steer-axle. This is because the roll stiffness of the steer-axle is far less than the other two, so it is the last one to lift off the ground.

1.2 What Has Been Done In The Rollover Research?

Previous research indicates that rollover accidents are strongly related to the basic roll stability of the vehicles. In a two-dimensional ("roll plane") model, the static rollover threshold, expressed as lateral acceleration in gravitational units (g), is the basic measure of roll stability. Research shows that the static rollover threshold of heavy trucks is lower than that of other vehicles and this appears to be the main reason for truck rollover accidents (Winkler, Blower, Ervin, 1999).

Virtually all rollover accidents in the real world are dynamic events to some extent. Research shows that the dynamic rollover threshold of heavy commercial vehicles in most cases is slightly less than or equal to the static rollover threshold of such vehicles and is relatively insensitive to steering maneuvers. The difference between the dynamic and static rollover threshold is less than 5%(Liu, Rakheja, Ahmed, 1998). So, the static rollover threshold is widely employed to estimate the dynamic rollover propensity of heavy vehicles in two-dimensional models.

In recent years, some so-called intelligent systems either on-board the vehicle or within the highway infrastructure have been fabricated based on the heavy vehicle rollover research (Rakheja, Piche, 1990; Lin, Cebon, Cole, 1996). Most on-board warning systems are based on the two-dimensional model and use the static rollover threshold as a warning reference parameter.

1.3 Three-Dimensional Models And Two-Dimensional Models

When a three-dimensional (3-D) trailer is modeled as a two-dimensional (2-D) unit vehicle, some rolling properties of trucks have been ignored.

From Figure 1.1, we can see the difference between the 2-D model and the 3-D trailer models. In (a) of Figure 1.1, the 2-D model indicates that roll of the cargo box is around a straight line parallel to the ground and passing through the rear suspension roll center P. In the 2-D model, the movement of cargo in the fore-aft direction is all the same and cannot be calculated separately. The influence of fore-aft parameters on the roll stability cannot be found either.

But from (b), we find that trailer cargo box actually rotates around an oblique line that passes through the fifth-wheel A and the rear suspension roll center P and is generally not parallel to the ground. If there are some moving cargos in the cargo box,

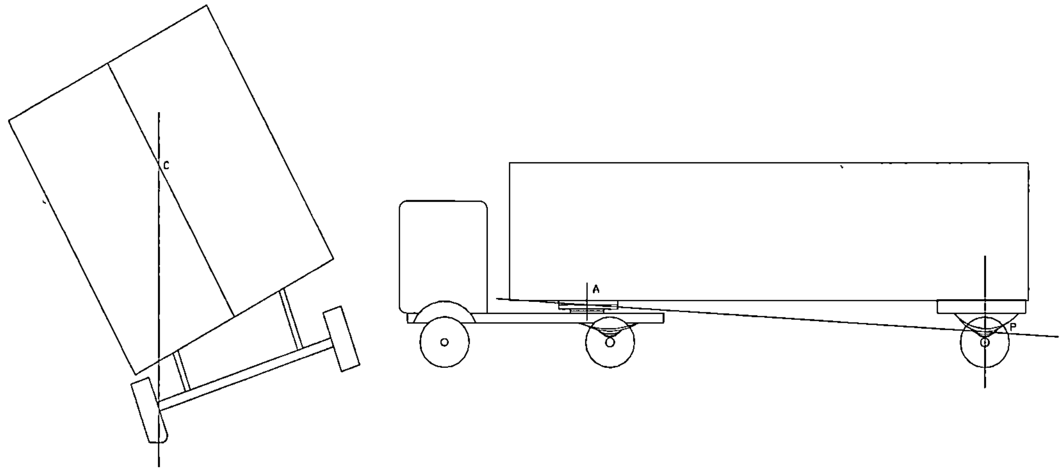

(a) (b)

Fig. 1.1 The Roll of Vehicles in Different Models

their movement in the fore-aft direction can be found separately. The influence of fore-aft parameters on the roll stability can also be found.

From the above discussion, we find that in the simulation of the rollover of heavy trucks, a 2-D model is not as accurate as a 3-D model, which better approximates the real trailer dynamics.

1.4 Roll Angle, Vehicle Speed And Lateral Acceleration

In a 2-D model, the lateral acceleration, which is referred to as the static rollover threshold, serves as the indicator of rollover or liftoff. In a 3-D model, the movement of the center of gravity is not only toward outside and upward, but backward too if the rolling around the oblique axis is considered. So the lateral acceleration of the center of gravity of the cargo box is no longer "lateral" in a 3-D model and is not a good criterion for rollover or liftoff.

Trucks are prone to rollover when exceeding a critical cornering speed (Francis, Navin, 1992). In a 3-D model, roll angle has proved to be a good indicator of rollover or liftoff, and vehicle speed is a good indicator of when the critical values of roll angle are reached. When the vehicle reaches roll angle ψ_1 at a certain speed, the trailer axle will lift off the ground. When it reaches roll angle ψ_2 at another speed, the drive axle will lift off the ground and rollover will happen. Though roll angle indicates when the liftoff and rollover will happen, vehicle speed determines when these roll angles will be reached. And vehicle speed is then the indirect indicator of liftoff and rollover. As the vehicle speed changes when liftoff or rollover happens, it indicates the change of roll stability of the vehicle. Like the lateral acceleration in the 2-D model, vehicle speed and roll angle are easy to measure in the 3-D model and make them good criteria for predicting rollover or liftoff.

1.5 Liftoff And Rollover

On most of the on-board warning systems, some measure of rollover threshold is used to warn the driver of a possible rollover. In other words, current warning systems are based on predicting the beginning of the second phase of rollover—the liftoff of drive-axle tires. But as discussed earlier in section 1.1, the process between liftoff and rollover depends on many influencing factors. Rollover may happen well before it is expected, or it may not happen when it is expected. Once the threshold point is reached, the vehicle loses its stability and rollover cannot be prevented. The focus of this thesis is to begin to evaluate the feasibility of a different warning strategy. In this new approach, warning would be based on predicting the beginning of the first phase of rollover—liftoff of the trailer tires. If a system warns of liftoff of the trailer tires when the truck is still stable, instead of warning that the truck has lost its stability, the driver (or an automated control system) might have more time and more opportunity to prevent the rollover from happening.

In this thesis, a simple three-dimensional dynamic model for a trailer of a five-axle heavy truck is established to predict the liftoff of trailer tires.

Chapter 2

Literature Review

In the 1970's, a number of investigators have studied the static and steady turning roll stability of articulated vehicles. In the late 1970's and early 1980's, roll stability of heavy duty trucks and truck combinations is discussed both on the level of the fundamental mechanics of vehicle response and from the viewpoint of the quantitative influence of various parameters.

Segel and Ervin (1981) were concerned with the influence of tire factors on truck stability. They concluded (a) that the fore/aft roll stiffness distribution was the primary mechanism serving to aggravate the yaw stability of the heavy truck, (b) that the commercial vehicle tire was seen to exhibit certain shear-force related properties that cause trucks to respond to parametric variations differently than typical passenger cars, and (c) that a marked degradation in directional controllability can accrue well in advance of the maneuver severity required to roll over the vehicle.

Mallikarjunarao and Ervin (1982) wrote a simulation model to determine rollover threshold of trucks in different size and weight configurations. This model, which is called the static roll model, provided a nonlinear treatment of the rolling motion of a vehicle that is composed of a maximum of three suspension sets. Thus a five-axle tractor- semitrailer is treated as three-axle tractor-semitrailer by combining the tandem axle pairs into single axle equivalents. This model can be used in all calculations except those involving the laterally offset load cases. The model works "backwards" in the sense that the user inputs a value of trailer roll angle and assumes static equilibrium in solving for the lateral acceleration condition needed to achieve that roll angle. The model incorporated such features as spring lash, lash in the fifth wheel coupling, torsional compliance of the tractor frame, and specified force/deflection properties and roll centers at each axle position. The sequential lift-off of wheels at the various axle positions is determined, also the rolling of the cab mass as well as the trailer mass. Each full trailer is treated as a single rigid body supported by two suspension assemblies.

Mallikarjunarao and Segel (1981) wrote another simulation model, called the yaw/roll model. It is a time-domain nonlinear simulation that can represent as many as three trailing units behind a tractor and as many as eleven axles in the combined vehicle. All of the features cited above for the static roll model are represented, in addition to a five-degree-of-freedom treatment of each rigid body, permitting evaluation of the total response to steering input.

Ervin (1983) also discussed the influence of heavy truck size and weight variables on the roll stability and concluded the lowering the center of gravity, raising the roll center, widening the track of the vehicle, increasing tire or suspension stiffness, decreasing suspension lash, and stiffening the drive-axle and steer-axle suspension all improve stability. Also, roll stability is optimized when load is distributed among suspensions in proportion to the distribution of roll stiffness. Later, Ervin (1986) further explored the dependence of truck roll stability on size and weight variables. In that paper, loading convention was noted and discussed in detail, and much truck data was provided.

MacAdam(1982) studied the two models above. He found that these models focused on the development of yaw divergence within the sub-limit maneuvering range and that the vehicles examined possessed centers of gravity heights that would be classified as moderate. In contrast, the computer based results presented in MacAdam's paper focus on the development of yaw divergence and/or roll instability for trucks possessing high centers of gravity, operating at low levels of lateral acceleration. The principal mechanism responsible for such behavior is shown to be the nonlinear variation of truck tire cornering stiffness with vertical load, acting in conjunction with typical, heavy truck fore/aft roll stiffness distributions. A simplified analysis of yaw stability was provided with assumes typical truck tire cornering stiffness variation with vertical load. Results from a comprehensive computer simulation were presented and the topic of close-loop driver control of yaw divergent vehicles, as represented by a computer model, were introduced and discussed.

Ervin, MacAdam and Barnes (1987) also studied the relationship between highway ramp geometries and vehicle dynamic behavior, and found that ramp design left a very small margin for control of the heavy vehicles because the maneuvering limits of trucks are lower than those of passenger cars.

Furleigh, Vanderploeg and Oh (1988) suggested that by designing four-wheel steering on heavy trucks, handling performance of the trailer at both high and low speed could be improved.

Laird (1988) studied the suspension properties of both tractor and trailer, including roll stiffness, roll center height, lateral compliance and suspension height, which influence roll stability. He found that increasing the roll center height and lowering suspension height of the trailer can improve the rollover moderately and that vehicle rollover is only slightly sensitive to trailer lateral compliance changes. Also, the gain achieved by lowering the suspension height will be lost if the distance between the trailer frame and the trailer floor is increased to maintain the trailer at the same height. If the frame-to-floor height is increased, effectively all that has been done is to lower the roll-center height, and consequently a reduction in rollover threshold occurs.

Miki (1988) made a five-mass model and found a method for evaluating stability and handling of a truck when torsional rigidity of the body is considered. The simulation results correspond well with the experimental results. This shows that evaluation of the influences of the body's torsional rigidity and the suspension's roll stiffness upon the stability and handling has become possible.

Bernard, Shannan and Vanderploeg (1989) discussed vehicle rollover on smooth surfaces. The paper presents various mathematical models that bear on rollover, starting with a very simple quasi-static model that requires knowledge of only a few measured vehicle parameters. It then deals with simulations of increasing complexity and increasing need for measurements to provide accurate and detailed input data.

In the 1990's, modern electronics are beginning to be applied to the problem of heavy vehicle rollover in the form of so-called intelligent systems either on-board the vehicle or within the highway infrastructure.

Fakheja and Piche (1990) developed a microprocessor based early warning safety device that can detect and warn the drivers of impending dynamic instabilities to improve the operational safety of articulated freight vehicles. This is one approach that is aimed at reducing the occurrence of commercial vehicle rollover through on board systems and was advertised for application on commercial vehicles as early as the late 1980s.

Winkler, Karamihas and Bogard (1992) discussed the roll stability performance of heavy vehicle suspensions because suspension properties play an important role in determining the roll stability of the commercial vehicle. The paper discussed the basic mechanisms of static roll stability and highlighted the role of suspension properties, especially roll stiffness, and roll center height and lateral stiffness, in establishing the roll stability limit. Much heavy vehicle suspensions data are presented.

Navin (1992) outlined the relative precision of equations of varying complexity used to estimate truck critical rollover speed based on tire marks. He found that the formulation to estimate a heavy, loaded vehicle's rollover lateral acceleration threshold need only include the height to the center of the mass, the lateral position of the center of mass suitably corrected for tire stiffness, and the road's super elevation. He also suggested that the current procedure of designing a highway to a standard and assuming an acceptable level of safety is not adequate in present-day engineering.

El-Gindy (1992) studied the use of a set of safety-related performance measures to control the dynamic quality of heavy vehicles from a design and regulatory standpoint. The study indicates that a set of safety-related performance measures could be beneficially introduced into the current process of designing and manufacturing vehicles and should be directed towards "married combinations", i.e., including the concept that a tractor should be identified to tow specific trailers.

Das, Suresh and Wambold (1993) developed a hybrid approach to determine the dynamic vehicle rollover threshold. The approach uses a roll plane vehicle model and a simulation based on testing that was carried out at low speeds, where lateral acceleration is measured. Curve-fitting techniques are used to extrapolate for the threshold values of lateral acceleration and forward velocity. This approach gives an objective measurement of dynamic rollover threshold of a vehicle in terms of lateral acceleration and velocity, making it possible to discriminate between vehicles of the same class.

El-Gindy, Tong and Tabarrok (1993) applied the frequency response method to predict the lateral acceleration at the center of gravity of each articulated vehicle unit and the rearward amplification ratio of Canadian logging trucks. A new yaw/ plane model was developed and used. The study found that the rearward amplification ratio trends displayed by vehicles employing jeeps or a pole trailer without a dolly are similar to the reference articulated vehicles. They also found that though the frequency response analysis is usually not sufficient to fully characterize the behavior, it does give a good understanding of the directional response of the vehicles.

Lin, Cebon and Cole (1996) describe an investigation into active roll control of articulated vehicles. This is another way to reduce the occurrence of commercial-vehicle rollover through on board systems and is the most direct method. They use active anti-roll bars and low bandwidth hydraulic actuators to minimize lateral load transfer effectively. They developed a nonlinear articulated vehicle model, simplified it with a linear articulated vehicle model and used it to choose gains for an active roll control system with a lateral acceleration controller. Using this model, they derived a relationship between the proportional gain of the tractor and trailer based on equal steady state load transfer of both units and reduced the peak transient load transfer significantly. This considerably improved the safety of the vehicle.

Liu, Rakheja, and Ahmed (1997) analyzed the relative rollover conditions of a heavy vehicle to establish an array of potential dynamic rollover indicators towards development of an early warning device. A relative roll instability indicator defined as Roll Safety Factor (RSF) is proposed and shown to be a highly reliable indicator regardless of vehicle configurations and operating conditions. Using a comprehensive directional dynamic analysis model, the factor was proved to be a good indicator for potential rollover. And a combination of all rollover indicators can be employed for application in an early warning system.

McFarlane, Sweatman, and Dovile (1997) explored the correlation of heavy vehicle performance parameters and found that there is some degree of correlation between the various performance attributes. Using correlation analysis may simplify the task of legislating performance standards.

E. Dahlberg and N. G. Vagstedt (1997) developed a simple 9-DOF generic articulated heavy vehicle model to study handling characteristics. This model possesses the ability of performing real time simulation up to the limits of yaw and roll stability. Its simplicity derives advantages of offering effective parameter variation possibilities in calculating handling characters such as lateral acceleration, yaw rate and load transfer.

Liu, Rakheja, and Ahmed (1998) studied the dynamic rollover threshold of the vehicle, derived for different suspension properties and operating conditions, and compared with the corresponding static rollover threshold of the vehicle. From the results of the study, it is established that dynamic rollover threshold based on effective lateral acceleration in most cases is either slightly lower or equal to the static rollover threshold acceleration and is relatively insensitive to steering maneuvers. The difference between the dynamic and static rollover is less than 5% for the vehicle configurations and the steering maneuvers considered in the study. The static rollover threshold may thus be conveniently employed to estimate the dynamic rollover propensity of heavy vehicles.

Winkler, Blower, and Ervin (1999) reviewed the state-of-the-art understanding of rollover of the commercial vehicle, presented accident statistics and the physical and statistical evidence for the linkage between vehicle roll stability and the actual occurrence of rollover accidents. The fundamentals of static roll stability are described in detail and then enhanced with discussion of dynamic considerations of the rollover process. The text concludes with a discussion of the evolving use of intelligent electronic systems and active vehicle control for reducing the occurrence of rollover.

Chapter 3

Three-Dimensional Trailer Steady Turning Liftoff Model

3.1 Three-Dimensional Trailer Model And Motion Equation

Consider the motion of a trailer shown in Fig 3.1. Let the trailer be modeled as two rigid bodies, referred to hereafter as the cargo box and the undercarriage and joined at a single point P.

Let there be neither pitch nor yaw of the cargo box relative to the undercarriage. In the following discussion, the axles of the undercarriage remain parallel to the road's surface. (That is, compliance of the trailer tires and suspension is neglected.)

The forces and moments of the two rigid bodies are shown in Fig 3.2 when there is a rolling movement of the cargo box relative to the undercarriage.

When the cargo box is empty or contains only fixed cargo, moment summation about the fifth wheel A gives

(3.1) $\quad \Sigma \overline{M}_A = \bar{r}_{AP} \times \overline{F}_P + \bar{r}_{AC} \times \overline{W}_C - \overline{M}_P .$

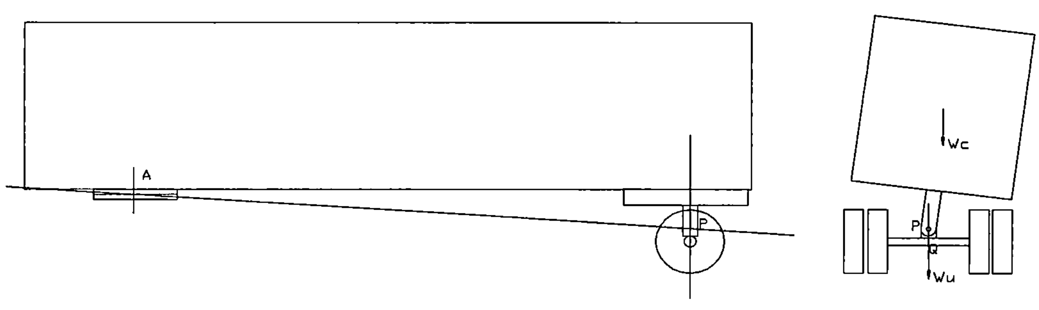

Fig 3.1 Two Rigid Body Model

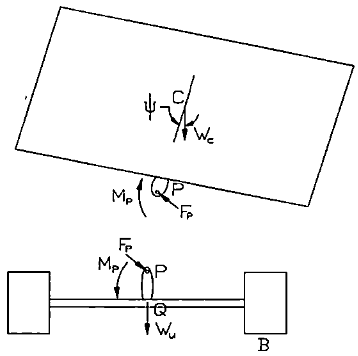

Fig 3.2 Free Body Diagram For The Trailer

Suppose that the tires on one side of the undercarriage lift off the ground, while the tires on the other side of the undercarriage maintain line contact with the road. Then on the undercarriage, moment summation about the contact line, which intersects the plane of Figure 3.2 at point B, gives

$$(3.2) \qquad \Sigma \overline{M}_B = \overline{M}_P + \overline{r}_{BP} \times \left(-\overline{F}_P\right) + \overline{r}_{BQ} \times \overline{W}_U .$$

Adding the two moment summations eliminates the moment at P, so that

$$\Sigma \overline{M}_A + \Sigma \overline{M}_B = \overline{r}_{AB} \times \overline{F}_P + \overline{r}_{AC} \times \overline{W}_C + \overline{r}_{BQ} \times \overline{W}_U .$$

The scalar product of $\overline{r}_{AB}$ with both sides of the equation eliminates the force at P to give

$$(3.3) \qquad \left(\Sigma \overline{M}_A + \Sigma \overline{M}_B\right) \cdot \overline{r}_{AB} = \left(\overline{r}_{AC} \times \overline{W}_C + \overline{r}_{BQ} \times \overline{W}_U\right) \cdot \overline{r}_{AB}$$

From rigid body dynamics (Ginsberg, 1995), moment summations at A and B are

$$(3.4) \qquad \Sigma \overline{M}_A = \dot{\overline{H}}_C + \overline{r}_{AC} \times m_C \overline{a}_C ,$$

$$(3.5) \qquad \Sigma \overline{M}_B = \dot{\overline{H}}_Q + \overline{r}_{BQ} \times m_U \overline{a}_Q .$$

The angular momentum of the cargo box and the undercarriage and their first derivatives with respect to time are

(3.6) $$\overline{H}_C = I_C \cdot \overline{\omega}_C \,,\ \dot{\overline{H}}_C = \dot{I}_C \cdot \overline{\omega}_C + I_C \cdot \overline{\alpha}_C + \overline{\omega}_C \times (I_C \cdot \overline{\omega}_C),$$

(3.7) $$\overline{H}_Q = I_Q \cdot \overline{\omega} \,,\ \dot{\overline{H}}_Q = \dot{I}_Q \cdot \overline{\omega} + I_Q \cdot \overline{\alpha} + \overline{\omega} \times (I_Q \cdot \overline{\omega}).$$

Assume that the motions of the fifth wheel and the undercarriage are prescribed. Then it is convenient to express the acceleration of C in terms of the acceleration of A, to which

$$\overline{a}_C = \overline{a}_A + \overline{a}_{C/A}.$$

The ground is taken as an inertial reference frame. Then the acceleration of A can be expressed as

$$\overline{a}_A = \overline{\alpha}_C \times \overline{r}_{OA} + \overline{\omega}_C \times (\overline{\omega}_C \times \overline{r}_{OA}).$$

where O is a reference point fixed in the inertial reference frame. The acceleration of C relative to A is

$$\overline{a}_{C/A} = \overline{\alpha}_C \times \overline{r}_{AC} + \overline{\omega}_C \times (\overline{\omega}_C \times \overline{r}_{AC}).$$

Combining the above three equation gives the acceleration of C

(3.8) $$\overline{a}_C = \overline{\alpha}_C \times \overline{r}_{OC} + \overline{\omega}_C \times (\overline{\omega}_C \times \overline{r}_{OC}),$$

in which

(3.9) $$\overline{r}_{OC} = \overline{r}_{OA} + \overline{r}_{AC}.$$

The acceleration at Q can be expressed as

(3.10) $$\overline{a}_Q = \overline{\alpha} \times \overline{r}_{OQ} + \overline{\omega} \times (\overline{\omega} \times \overline{r}_{OQ}).$$

Substituting equations (3.4) to (3.10) into (3.3) gives

$$\begin{aligned}(3.11)\quad &\{I_C\cdot\overline{\alpha}_C+\overline{\omega}_C\times(I_C\cdot\overline{\omega}_C)+\dot{I}_C\cdot\overline{\omega}_C+\overline{r}_{AC}\times m_C[\overline{\alpha}_C\times\overline{r}_{OC}+\overline{\omega}_C\times(\overline{\omega}_C\times\overline{r}_{OC})-\overline{g}]\\ &+I_Q\cdot\overline{\alpha}+\overline{\omega}\times(I_Q\cdot\overline{\omega})+\dot{I}_Q\cdot\overline{\omega}+\overline{r}_{BQ}\times m_U[\overline{\alpha}\times\overline{r}_{OQ}+\overline{\omega}\times(\overline{\omega}\times\overline{r}_{OQ})-\overline{g}]\}\cdot\overline{r}_{AB}=0\end{aligned}$$

which is referred to herein as the first trailer motion equation and is valid for arbitrary motion.

Let the moment at P be represented by a torsional spring, so that

$$(3.12)\quad \overline{M}_P=\overline{k}\cdot\psi.$$

If we substitute (3.12) in (3.1) and take the dot product of both sides of the resulting equation with $\overline{r}_{AP}$, we find

$$\begin{aligned}(3.13)\quad &\overline{r}_{AP}\cdot\{I_C\cdot\overline{\alpha}_C+\overline{\omega}_C\times(I_C\cdot\overline{\omega}_C)+\dot{I}_C\cdot\overline{\omega}_C\\ &+\overline{r}_{AC}\times m_C[\overline{\alpha}_C\times\overline{r}_{OC}+\overline{\omega}_C\times(\overline{\omega}_C\times\overline{r}_{OC})-\overline{g}]+\overline{k}\cdot\psi\}=0\end{aligned}$$

which is referred to herein as the second trailer motion equation and is valid for arbitrary motion.

3.2 Steady Circular Steering Liftoff Equation

The specific motion considered in this thesis is steady turning. The path of the fifth wheel is assumed to be a circle in a horizontal plane. This can be achieved in practice by holding the tractor's steering angle constant. A further assumption is that the rear roll center, *P*, travels on the same circle as the fifth wheel. While this assumption must be approximately correct, it may introduce a measurable error. Determining the extent of that error is beyond the scope of this thesis.

Given the above assumptions regarding the motion of points *A* and *P* of the trailer, trailer roll and liftoff can be studied without modeling the tractor. Although the tractor would be need to produce the assumed motion of A and P, the assumptions alone are sufficient to determine the trailer's roll angle and liftoff speed.

Considering the relationship between the angular velocity of the cargo box and the undercarriage, we have for arbitrary motion

$$(3.14) \quad \overline{\omega}_C = \overline{\omega} + \overline{\Omega}$$

Similarly, the angular acceleration is separated as

$$(3.15) \quad \overline{\alpha}_C = \overline{\alpha} + \dot{\overline{\Omega}}.$$

In circular turning with constant velocity, the relative motion between the undercarriage and the cargo box is zero, so that

$$\overline{\Omega} = 0, \ \dot{\overline{\Omega}} = 0.$$

The angular acceleration of the undercarriage relative to the inertial reference frame is also zero, so that

$$\overline{\alpha} = 0.$$

Then (3.14) and (3.15) become

$$(3.16) \quad \overline{\omega}_C = \overline{\omega}, \ \overline{\alpha}_C = \overline{\alpha} = 0.$$

Taking (3.16) into (3.11) and (3.13) gives

$$(3.17) \quad \begin{aligned} &\overline{r}_{AB} \cdot \{\overline{\omega} \times [(I_Q + I_C) \cdot \overline{\omega}] + (\dot{I}_Q + \dot{I}_C) \cdot \overline{\omega} + \overline{r}_{AC} \times m_C[\overline{\omega} \times (\overline{\omega} \times \overline{r}_{OC}) - \overline{g}] \\ &+ \overline{r}_{BQ} \times m_U[\overline{\omega} \times (\overline{\omega} \times \overline{r}_{OQ}) - \overline{g}]\} = 0 \end{aligned}$$

$$(3.18) \quad \overline{r}_{AP} \cdot \{\overline{\omega} \times (I_C \cdot \overline{\omega}) + \dot{I}_C \cdot \overline{\omega}_C + \overline{r}_{AC} \times m_C[\overline{\omega} \times (\overline{\omega} \times \overline{r}_{OC}) - \overline{g}] + \overline{k} \cdot \psi\} = 0$$

which are steady turning motion equations for the trailer.

3.3 Plane Circular Steady Steering Equation

Suppose that the truck travels in a left turn on a circular path in a horizontal plane. Let $(\overline{e}_t,\overline{e}_n,\overline{e}_b)$ be a coordinate system fixed on the undercarriage and originating at point Q, such that when the undercarriage is horizontal, as shown in Fig 3.3

$\overline{e}_t$ = tangent to the path of Q,

$\overline{e}_n$ = perpendicular to $\overline{e}_t$ in the same level plane and pointing to the center of the curve (left when facing forward),

$\overline{e}_b$ = up.

On the other hand, define a moving unit vector system $(\overline{U}_1,\overline{U}_2,\overline{U}_3)$ originating at point P and fixed relative to the undercarriage such that when the cargo box is upright,

$\overline{U}_1$ = forward (directed from the rear of the trailer toward the front of the trailer),

$\overline{U}_2$ = port (left when facing forward),

$\overline{U}_3$ = up

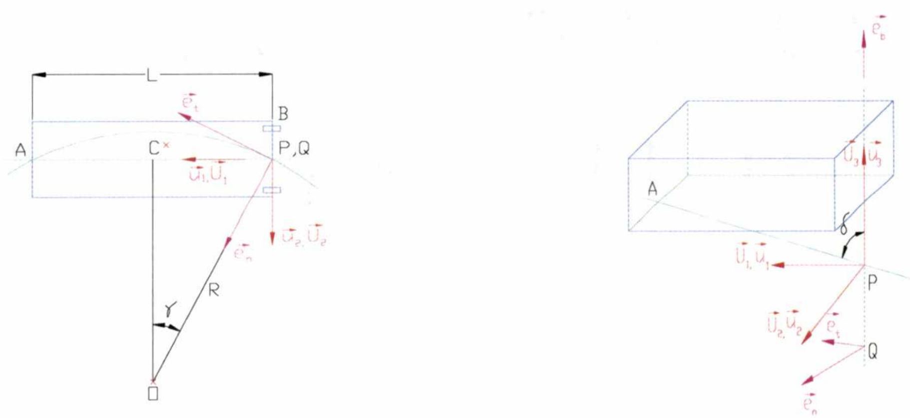

Fig 3.3 Definition Of Coordinate Systems On The Trailer

Let $(\bar{u}_1, \bar{u}_2, \bar{u}_3)$ be unit vectors fixed in the cargo box, initially aligned with the $(\bar{U}_1, \bar{U}_2, \bar{U}_3)$ system, and rotating with the cargo box.

All of the quantities in (3.17) and (3.18) will be expressed in the $(\bar{U}_1, \bar{U}_2, \bar{U}_3)$ system. Since that is a body-axis system for the undercarriage, $\dot{I}_Q = 0$. Since $\bar{\Omega} = 0$ and $\dot{\bar{\Omega}} = 0$, it follows that $\dot{\psi} = 0$, $\ddot{\psi} = 0$, and $\dot{I}_C = 0$. (3.17) and (3.18) then becomes

$$\begin{aligned} &\bar{r}_{AB} \cdot \{\bar{\omega} \times [(I_Q + I_C) \cdot \bar{\omega}] + \bar{r}_{AC} \times m_C[\bar{\omega} \times (\bar{\omega} \times \bar{r}_{OC}) - \bar{g}] \\ &+ \bar{r}_{BQ} \times m_U[\bar{\omega} \times (\bar{\omega} \times \bar{r}_{OQ}) - \bar{g}]\} = 0 \end{aligned} \tag{3.19}$$

$$\bar{r}_{AP} \cdot \{\bar{\omega} \times (I_C \cdot \bar{\omega}) + \bar{r}_{AC} \times m_C[\bar{\omega} \times (\bar{\omega} \times \bar{r}_{OC}) - \bar{g}] + \bar{k} \cdot \psi\} = 0 \tag{3.20}$$

which are plane circular steady turning motion equations for the trailer.

In equation (3.19) and (3.20), $\bar{\omega}$ can be defined as

$$\bar{\omega} = v \cdot \bar{\beta} \tag{3.21}$$

in which v is the velocity of the undercarriage, and $\bar{\beta}$ is the reciprocal of the three-dimensional radius or torsion of the path of the undercarriage. $\bar{\beta}$ is defined as

$$\bar{\beta} = \begin{Bmatrix} \dfrac{d\bar{e}_n}{ds} \cdot \bar{e}_b \\ \dfrac{d\bar{e}_b}{ds} \cdot \bar{e}_t \\ \dfrac{d\bar{e}_t}{ds} \cdot \bar{e}_n \end{Bmatrix}.$$

It follows that

$$\bar{\beta}^e = \begin{Bmatrix} \dfrac{1}{\tau} \\ 0 \\ \dfrac{1}{\rho} \end{Bmatrix}$$

in $\{\overline{e}_t, \overline{e}_n, \overline{e}_b\}$ system. Considering the relationship among $\overline{e}_n$, $\overline{e}_t$ and $\overline{e}_b$, we find that

$$\frac{d\overline{e}_t}{ds} = \frac{1}{\rho}\overline{e}_n,$$

$$\frac{d\overline{e}_n}{ds} = -\frac{1}{\rho}\overline{e}_t + \frac{1}{\tau}\overline{e}_b,$$

$$\frac{d\overline{e}_b}{ds} = -\frac{1}{\tau}\overline{e}_n.$$

Since we want to express equation (3.19) and (3.20) in system $(\overline{U}_1, \overline{U}_2, \overline{U}_3)$, we will transform $\overline{\beta}^e$ into the $(\overline{U}_1, \overline{U}_2, \overline{U}_3)$ system. The relationship between the two systems is

$$\begin{Bmatrix} \overline{U}_1 \\ \overline{U}_2 \\ \overline{U}_3 \end{Bmatrix} = R_{eb}(\gamma) \cdot \begin{Bmatrix} \overline{e}_t \\ \overline{e}_n \\ \overline{e}_b \end{Bmatrix},$$

where the transfer matrix $R_{eb}(\gamma)$ is

$$R_{eb}(\gamma) = \begin{bmatrix} \cos(\gamma) & \sin(\gamma) & 0 \\ -\sin(\gamma) & \cos(\gamma) & 0 \\ 0 & 0 & 1 \end{bmatrix}.$$

Then $\overline{\beta}$ in $(\overline{U}_1, \overline{U}_2, \overline{U}_3)$ is

$$\overline{\beta} = R_{eb}(\gamma) \cdot \overline{\beta}^e = \begin{Bmatrix} \frac{1}{\tau}\cos\gamma \\ -\frac{1}{\tau}\sin\gamma \\ \frac{1}{\rho} \end{Bmatrix}.$$

For plane circular steady state steering, $\tau \to \infty$ and $\rho = R$ in which R is the radius of the steering circle on which Q travels.

Then in plane circular steady steering, the angular velocity (3.21) is

$$(3.22) \qquad \overline{\omega} = v \cdot \begin{Bmatrix} 0 \\ 0 \\ \frac{1}{R} \end{Bmatrix} = \frac{v}{R} \cdot \overline{U}_3$$

in the $(\overline{U}_1, \overline{U}_2, \overline{U}_3)$ system.

In $(\overline{U}_1, \overline{U}_2, \overline{U}_3)$, the gravitational acceleration constant is

$$(3.23) \qquad \overline{g} = -g \cdot \overline{U}_3 .$$

The trailer suspension stiffness is

$$(3.24) \qquad \overline{k} = k_0 \cdot \overline{U}_1 .$$

In $(\overline{U}_1, \overline{U}_2, \overline{U}_3)$, if we assume that the mass of the undercarriage is distributed symmetrically with respect to the $\overline{U}_1, \overline{U}_3$ plane, the inertia tensor at Q can be written as

$$(3.25) \qquad I_Q = \begin{bmatrix} I_{Q11} & 0 & I_{Q13} \\ 0 & I_{Q22} & 0 \\ I_{Q31} & 0 & I_{Q33} \end{bmatrix}.$$

If the inertia tensor of C in the $(\overline{u}_1, \overline{u}_2, \overline{u}_3)$ system before any rolling is

$$I_C^0 = \begin{bmatrix} I_{C11} & I_{C12} & I_{C13} \\ I_{C21} & I_{C22} & I_{C23} \\ I_{C31} & I_{C32} & I_{C33} \end{bmatrix},$$

after a rolling of ψ around an arbitrary axis $\overline{PA}$, the inertia tensor at C in $(\overline{U}_1, \overline{U}_2, \overline{U}_3)$ becomes

$$(3.26) \qquad I_C = R_{U-u}{}^T \cdot I_C^0 \cdot R_{U-u} ,$$

in which R_{U-u} is the transform matrix from $(\overline{U}_1, \overline{U}_2, \overline{U}_3)$ to the body unit system $(\overline{u}_1, \overline{u}_2, \overline{u}_3)$ after the rolling of ψ,

$$R_{U-u} = R_{u2}(-(90-\delta))^T \cdot R_{u1}(\psi) \cdot R_{u2}(-(90-\delta)),$$

in which

$$R_{u2}(-(90-\delta)) = \begin{bmatrix} \cos(-(90-\delta)) & 0 & -\sin(-(90-\delta)) \\ 0 & 1 & 0 \\ \sin(-(90-\delta)) & 0 & \cos(-(90-\delta)) \end{bmatrix},$$

and

$$R_{u1}(\psi) = \begin{bmatrix} 1 & 0 & 0 \\ 0 & \cos(\psi) & \sin(\psi) \\ 0 & -\sin(\psi) & \cos(\psi) \end{bmatrix}.$$

The length vectors in $(\overline{U}_1, \overline{U}_2, \overline{U}_3)$ systems in Fig 3.4 respectively are

(3.27) $$\overline{r}_{AB} = \begin{Bmatrix} -L \\ -\dfrac{T}{2} \\ -q-d \end{Bmatrix}.$$

(3.28) $$\overline{r}_{AP} = \begin{Bmatrix} -L \\ 0 \\ -d \end{Bmatrix}.$$

(3.29) $$\overline{r}_{OQ} = \begin{Bmatrix} -\dfrac{L}{2} \\ -\sqrt{R^2 - \left(\dfrac{L}{2}\right)^2} \\ 0 \end{Bmatrix}.$$

(3.30) $$\overline{r}_{BQ} = \begin{Bmatrix} 0 \\ \dfrac{T}{2} \\ q-p \end{Bmatrix}.$$

$$(3.31)\quad \bar{r}_{OA} = \begin{Bmatrix} \dfrac{L}{2} \\ -\sqrt{R^2 - \left(\dfrac{L}{2}\right)^2} \\ d+p \end{Bmatrix}.$$

$$(3.32)\quad \bar{r}_{AC} = R_{U-u}{}^{T} \cdot \bar{r}^{\,0}_{AC},$$

in which

$\bar{r}^{\,0}_{AC} = \begin{Bmatrix} -a \\ t \\ h \end{Bmatrix}$ is the vector in $(\bar{u}_1, \bar{u}_2, \bar{u}_3)$ before its rolling of ψ around $\overline{PA}$.

$$(3.33)\quad \bar{r}_{OC} = \bar{r}_{OA} + \bar{r}_{AC}.$$

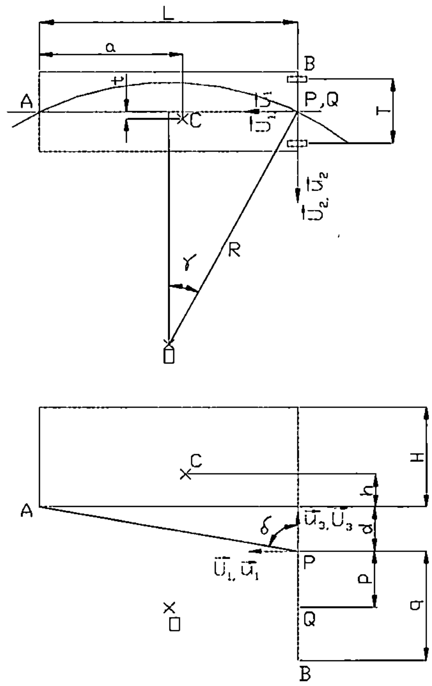

Fig 3.4 Definition Of Lengths And Angles On The Trailer

Substitution of equations (3.22) through (3.33) into equations (3.19) and (3.20) gives two liftoff equations that express the relationship among path radius R, longitude velocity v, and roll angle ψ at the instant of trailer liftoff. When liftoff happens at a certain path radius R, v and ψ are completely determined by these two liftoff equations. So the trailer speed v and the roll angle ψ are two indicators of liftoff at a certain path radius. Solving the nonlinear equation system (3.19) and (3.20) when R is given yields the trailer speed and roll angle at the instant of liftoff.

The model described above can be used to study liftoff for the trailer alone or for the trailer with arbitrary fixed cargo. If the trailer carries moving cargo (liquid or hanging cargo), the model must be modified.

Chapter 4

Results And Verification

4.1 Results

Equations (3.19) and (3.20) express the relationship among three liftoff parameters: the liftoff speed v, the roll angle at liftoff ψ and the path radius R. When the trailer is moving around a circle for which the radius R is known, the speed v and the roll angle ψ are certain values when the liftoff happens. So, the calculation results focus mainly on the influence of pertinent mechanical properties of the trailer on the liftoff parameters.

All of the results presented below were computed using realistic values for geometric and inertial properties of a semi-trailer and its cargo. These data are listed in the Appendix, and most were taken from " A Factbook of the Mechanical Properties of the Components for Single-Unit and Articulated Heavy Trucks" written by Fancher, Ervin, Winkler and Gillespie in 1986. The only exceptions to this are the pitch and yaw moments of inertia for the undercarriage. Since no data was available for them, they were computed using estimated radii of gyration. In what follows, the "unloaded" and "loaded" conditions refer to an empty cargo box and a cargo box loaded with the fixed cargo described in the Appendix, respectively. The center of gravity of the cargo was assumed to be at the same elevation as that of the empty cargo box.

4.1.1 Influence Of Path Radius *R*

When the path radius R is known, the trailer speed v and the roll angle ψ at liftoff are both determined by the liftoff equations, (3.19) and (3.20). As shown in Fig 4.1, liftoff speed increases when path radius increases in steady state turning. So it is wise to make a wide turn in cornering or lane changing maneuver.

When the steering path radius is 1000 m, the liftoff speeds are 72.988 m/s (164.22 mph) and 60.77 m/s (136.73 mph) for unloaded and loaded trailer respectively. That means liftoff is almost impossible for this trailer when the path radius reaches 1000 meters in steady state turning. When the trailer is loaded, its liftoff speed is lower and liftoff is more likely to happen than it is for the unloaded trailer.

Fig. 4.2 indicates that the liftoff roll angle ψ increases slightly when path radius R increases for the unloaded trailer. The roll angle change is just from 1.5082° to 1.5085° when the steering radius changes from 100 meters to 1000 meters. Fig 4.3 indicates that for the partially loaded trailer, if a 500-lbf cargo is added, the roll angles at liftoff remain unchanged at 2.073°. Fig 4.4 indicates that for the fully loaded trailer, a slight decrease from 7.0071° to 7.0051° for the same radius change is found. It is noteworthy that the amount of load affects the trend of the change of the roll angle at liftoff, and that the liftoff angle changes from increasing to decreasing when path radius increases. At this point, we have no simple, intuitive explanation for this phenomenon. But if the amount of change of liftoff roll angle is considered, we find that the differences are only 0.020%, 0.00% and 0.029%, respectively, for the unloaded, partially loaded and fully loaded trailers. So, we can safely say that for the three configurations used here, liftoff roll angle ψ does not change significantly with path radius R. This suggests that the roll angle may be a good indicator of impending liftoff. (To establish whether this be true, one

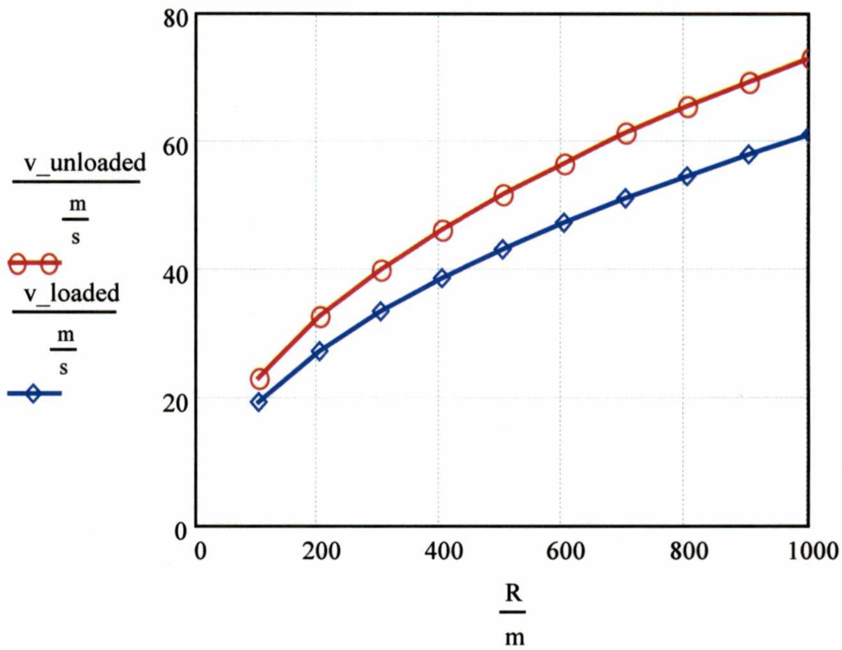

Fig 4.1 Change Of Liftoff Speed v With Path Radius R

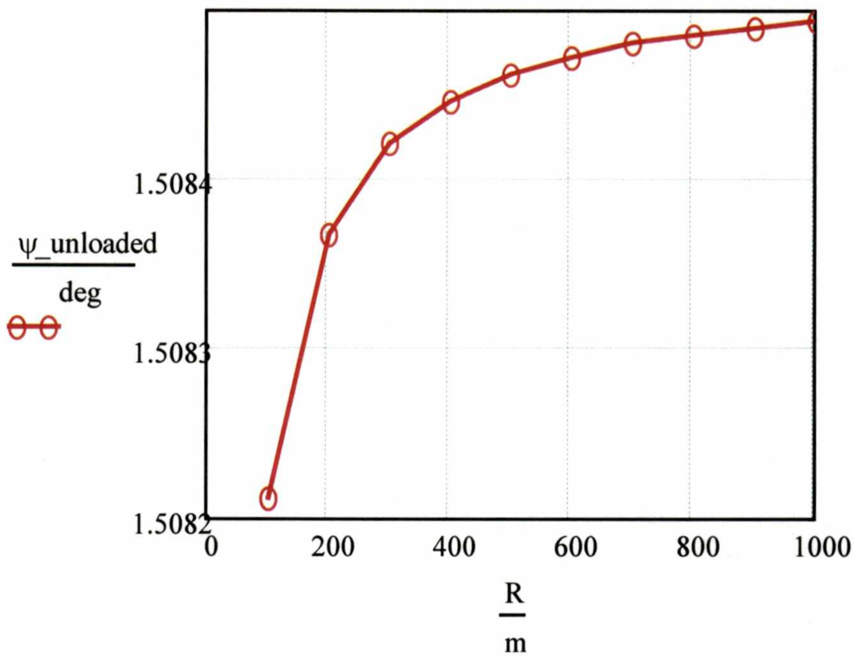

Fig 4.2 Change Of Liftoff Roll Angle ψ With Path Radius R For Unloaded Trailer

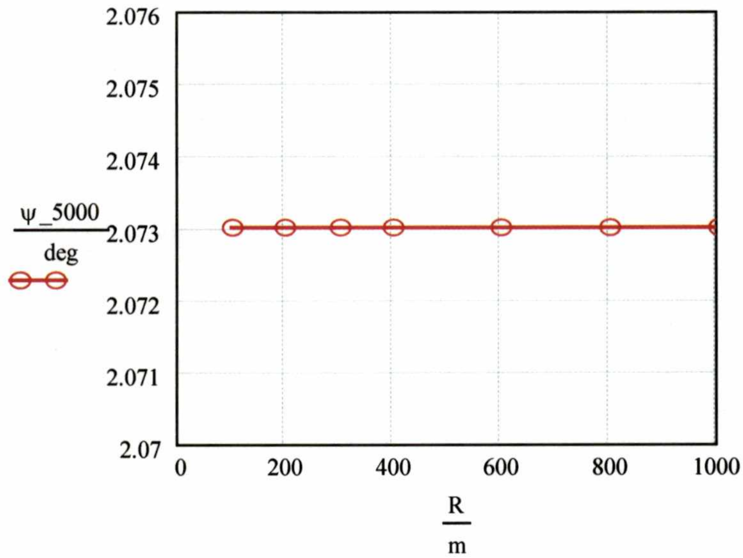

Fig. 4.3 Change Of Liftoff Roll Angle ψ With Path Radius R For Partially Loaded Trailer (W_load=5000 lbf)

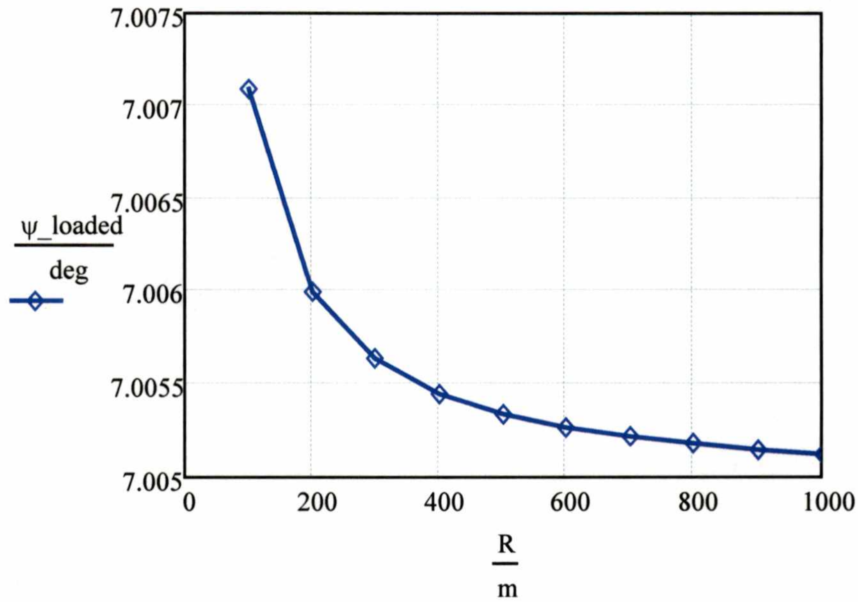

Fig. 4.4 Change Of Liftoff Roll Angle ψ With Path Radius R For Loaded Trailer

would need to simulate the trailer's roll angle at speeds lower than the liftoff speed. That is beyond the scope of this thesis.). When the roll angle of the trailer cargo box reaches the calculated value for a certain trailer configuration, there is potential danger of liftoff. When the vehicle speed reaches the calculated liftoff speed, the liftoff will then happen. But there are many mechanical properties that can affect the liftoff and roll stability of trailers. These will be discussed later in this chapter.

4.1.2 The Influence Of The Geometric Layout Of The Trailer

4.1.2.1 The Influence Of The Trailer Track Width *T*

Track width is one of the most fundamental vehicle properties that influence basic roll stability. As shown in Fig 4.5 and Fig 4.6, as the track width becomes larger, liftoff speed and roll angle will both increase. When the path radius is 500 meters, the trailer is unloaded, and the track width changes from 62 in to 82 in, the liftoff speed increases from 47.89 m/s to 55.08 m/s. For a loaded trailer, the change is 39.85 m/s to 45.90 m/s. The roll angle change is from 1.30° to 1.72° for an unloaded trailer. For a loaded trailer, the roll angle change is from 6.04° to 7.97°. So, increase in track width constitutes a powerful means of increasing roll stability. Unfortunately, the limitations of highway construction prohibit practical application of this fact.

From Fig 4.6, we can also find that when the trailer is loaded, the influence of track width is larger. The roll angle change for the loaded trailer is about 2°, but the change for the unloaded trailer is less than 0.5°. So, wider track width is especially beneficial to heavier trucks.

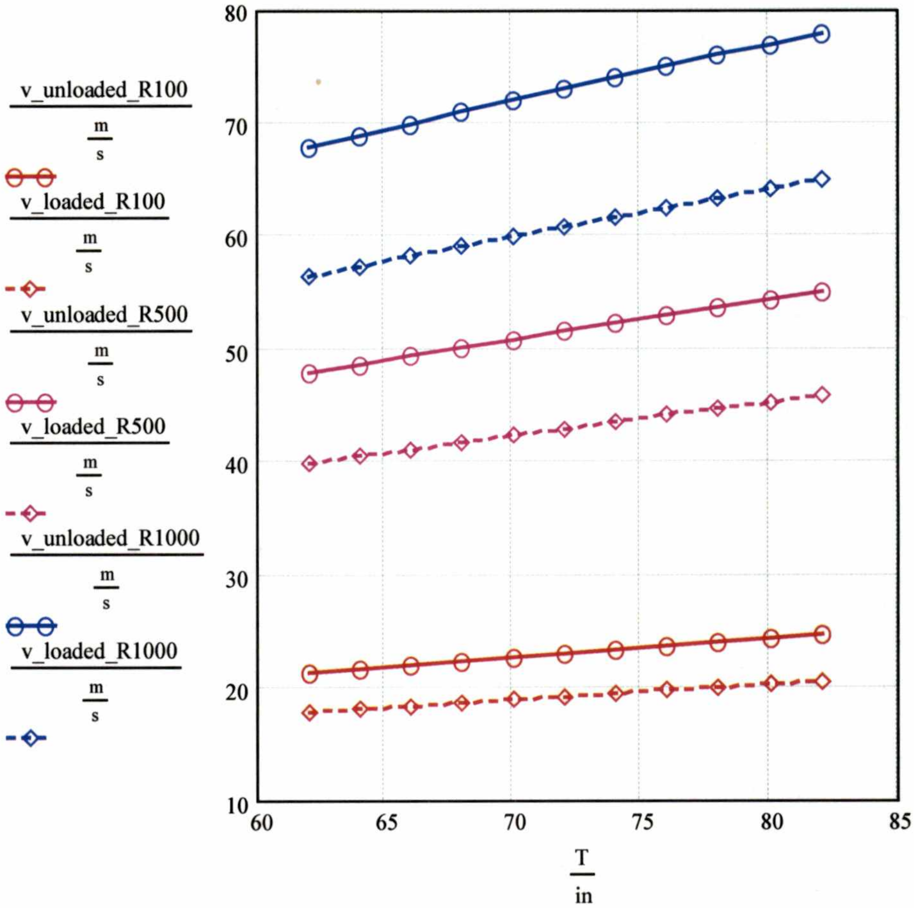

Fig 4.5 Change Of Liftoff Speed *v* With Track Width *T*

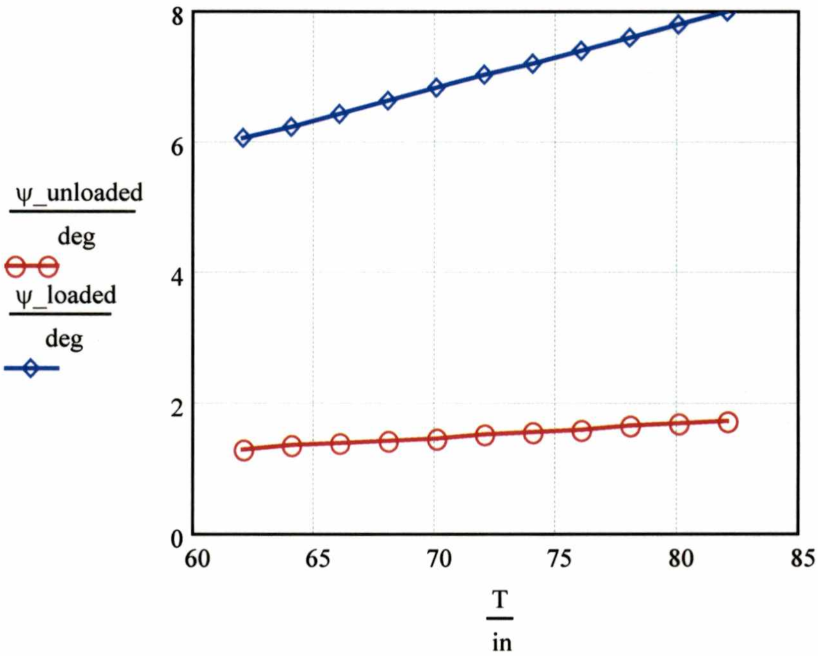

Fig 4.6 Change Of Liftoff Roll Angle ψ With Track Width T

4.1.2.2 The Influence Of The Roll Center Height q

Keeping the fifth wheel height $q+d$ unchanged while changing the roll center height q, reveals the influence of the roll center height on the liftoff of the trailer.

From Fig 4.7, we find that when the trailer is loaded, the liftoff speed will increase when the roll center is higher. But if the trailer is unloaded, the liftoff speed decreases when the roll center is higher. When the truck travels on a circle with radius of 500 meters, and when the roll center height changes from 19 in to 39 in, the speed change is from 52.56 m/s to 50.67 m/s for the unloaded trailer and from 41.52 m/s to 44.16 m/s for the loaded trailer.

From Fig 4.8, we find that with higher roll center, the liftoff roll angle decreases for both the loaded and unloaded trailers. When the trailer travels on a 500 m circle and the roll center height changes from 19 in to 39 in, the change in liftoff roll angle is from 1.86° to 1.18° for the unloaded trailer and from 8.17° to 5.74° for the loaded trailer, respectively. So, for a loaded trailer, higher roll center serves to improve liftoff and roll stability.

4.1.2.3 The Influence Of The Fifth Wheel Height $q+d$

We can find the influence of the fifth wheel height on liftoff of the trailer by changing the distance, d, between the roll center and the fifth wheel. At the same time, we change the center of gravity height h to keep the distance between the roll center and the cargo box center of gravity, $d+h$, unchanged.

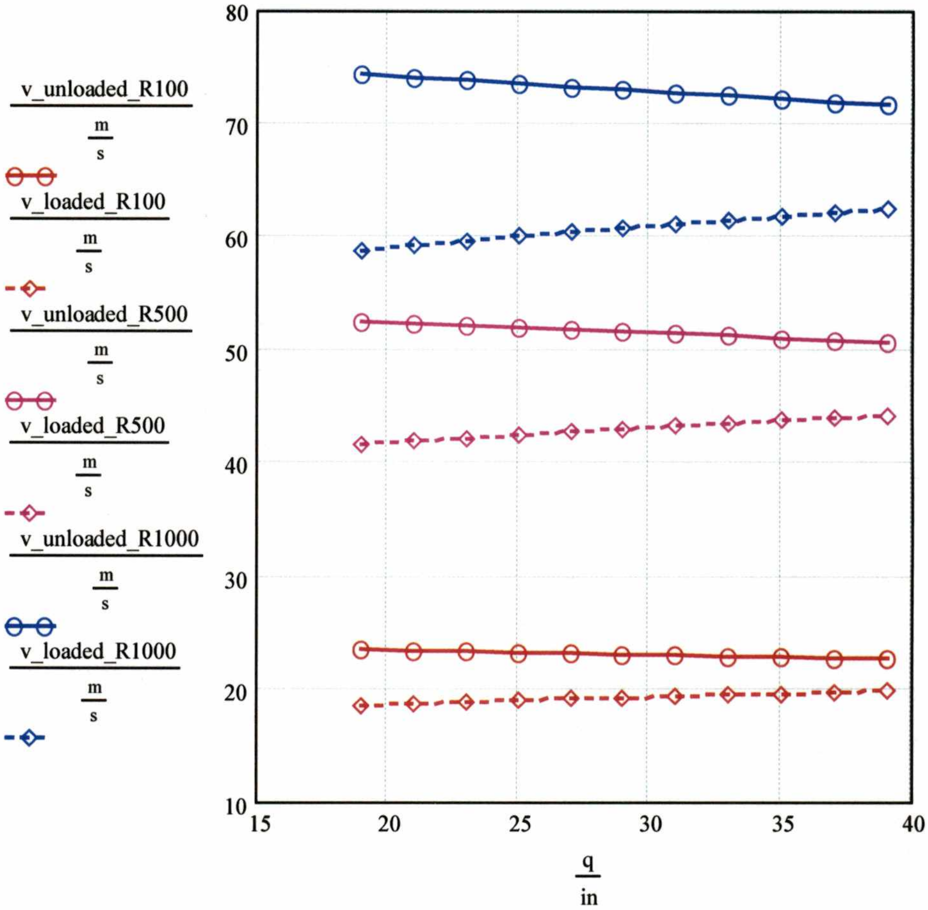

Fig 4.7 Change Of Liftoff Speed *v* With Roll Center Height *q*

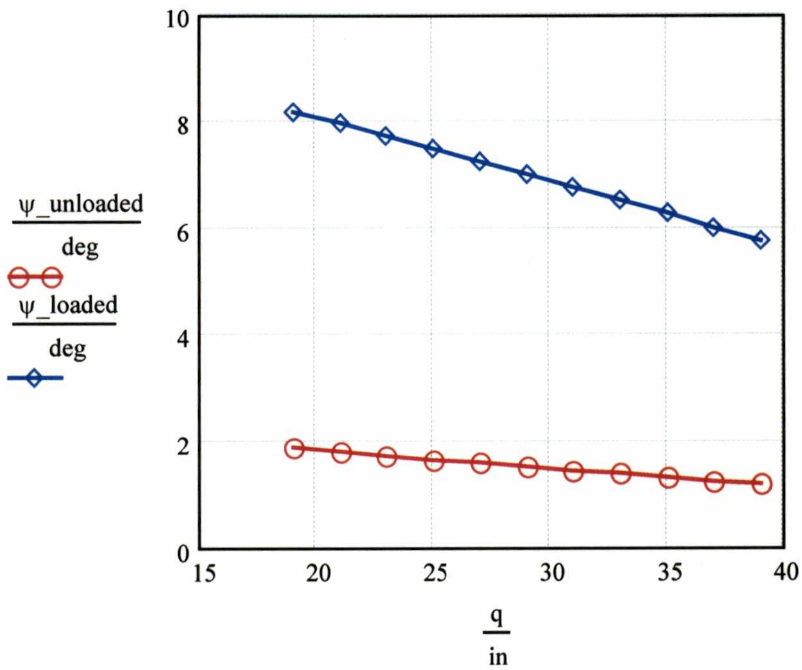

Fig 4.8 Change Of Liftoff Roll Angle ψ With Roll Center Height q

From Fig 4.9 and Fig 4.10, we find that liftoff speed increases when the fifth wheel is higher; but the liftoff roll angle decreases slightly at the same time. When rotating around a circle with radius of 500 meters, the speed change is from 49.87 m/s to 53.53 m/s for the unloaded trailer and from 40.85 m/s to 45.27 m/s for the loaded trailer when distance *d* changes from 10 in to 30 in.

From Fig 4.10, we find that with higher fifth wheel, the liftoff roll angle decreases slightly for both loaded and unloaded trailer. For a trailer rotating around a 500-meter circle, changing *d* from 10 in to 30 in changes the liftoff roll angle from 1.57° to 1.43° for the unloaded trailer and from 7.29° to 6.68° for the loaded trailer.

From the results described above, we conclude that a higher fifth wheel increases liftoff speed and decreases liftoff roll angle slightly. Thus, a higher fifth wheel improves the liftoff and roll stability. But its influence on roll stability is slight.

4.1.2.4 Influence Of The Suspension Roll Stiffness *k*

In this model, only the roll stiffness of the trailer axle is considered. Its influence on liftoff can be found from Fig 4.11 and 4.12.

We find that liftoff speed increases when the roll stiffness is higher; but the liftoff roll angle decreases when the roll stiffness is higher. For a trailer rotating around a circle with a radius of 500 meters, changing roll stiffness from 9,0000 in·lbf/deg to 19,0000 in·lbf/deg changes liftoff speed from 51.19 m/s to 51.8 m/s for the unloaded trailer and from 40.20 m/s to 44.16 m/s for the loaded trailer. So, the influence of the roll stiffness is more significant when the trailer is loaded.

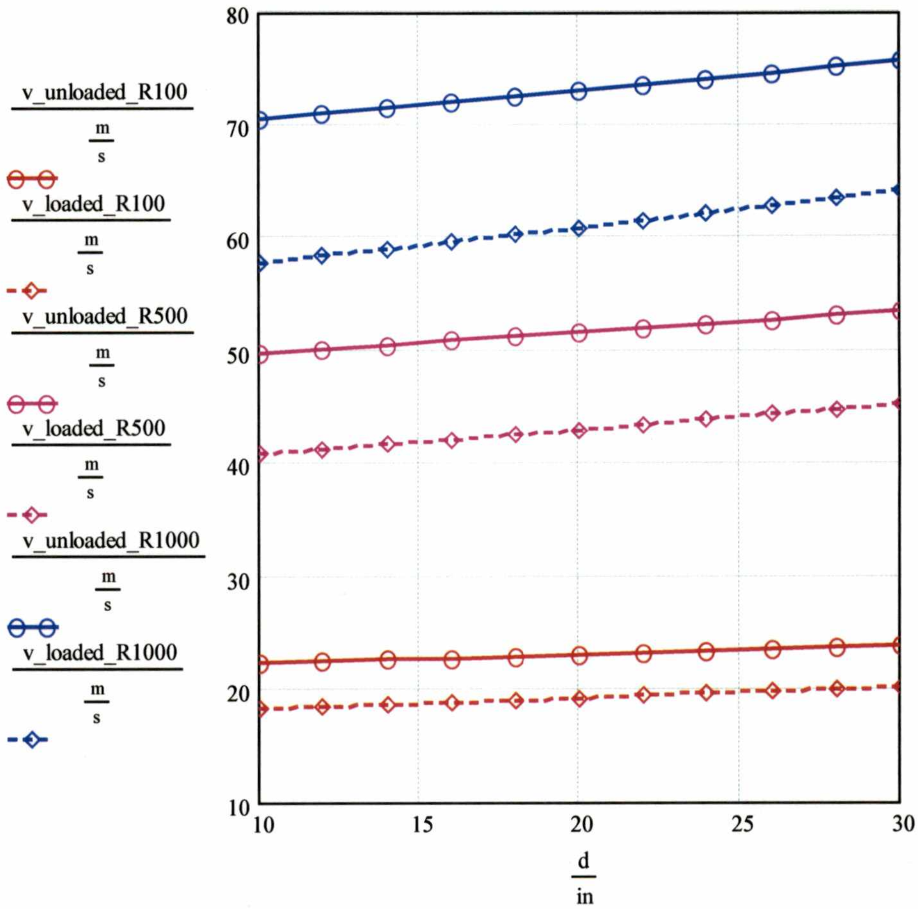

Fig 4.9 Liftoff Speed *v* Change With Fifth Wheel Height *q*+*d*

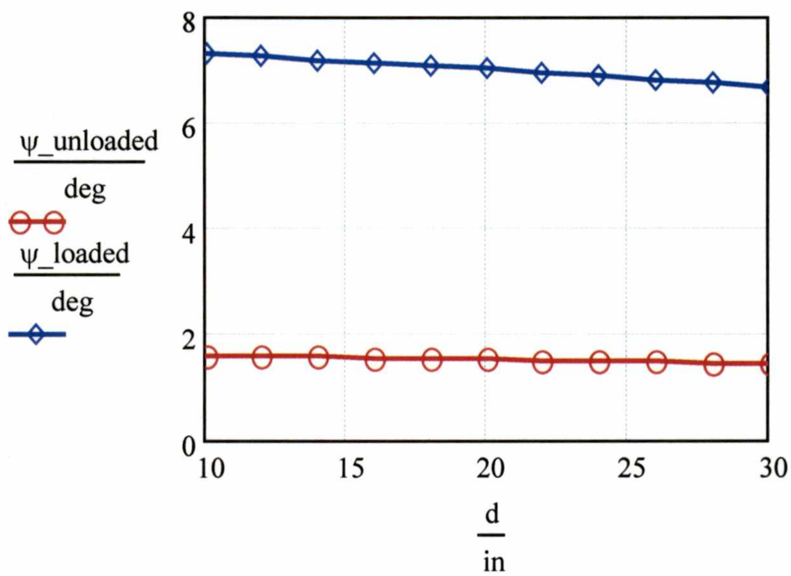

Fig 4.10 Liftoff Roll Angle ψ Change With Fifth Wheel Height $q+d$

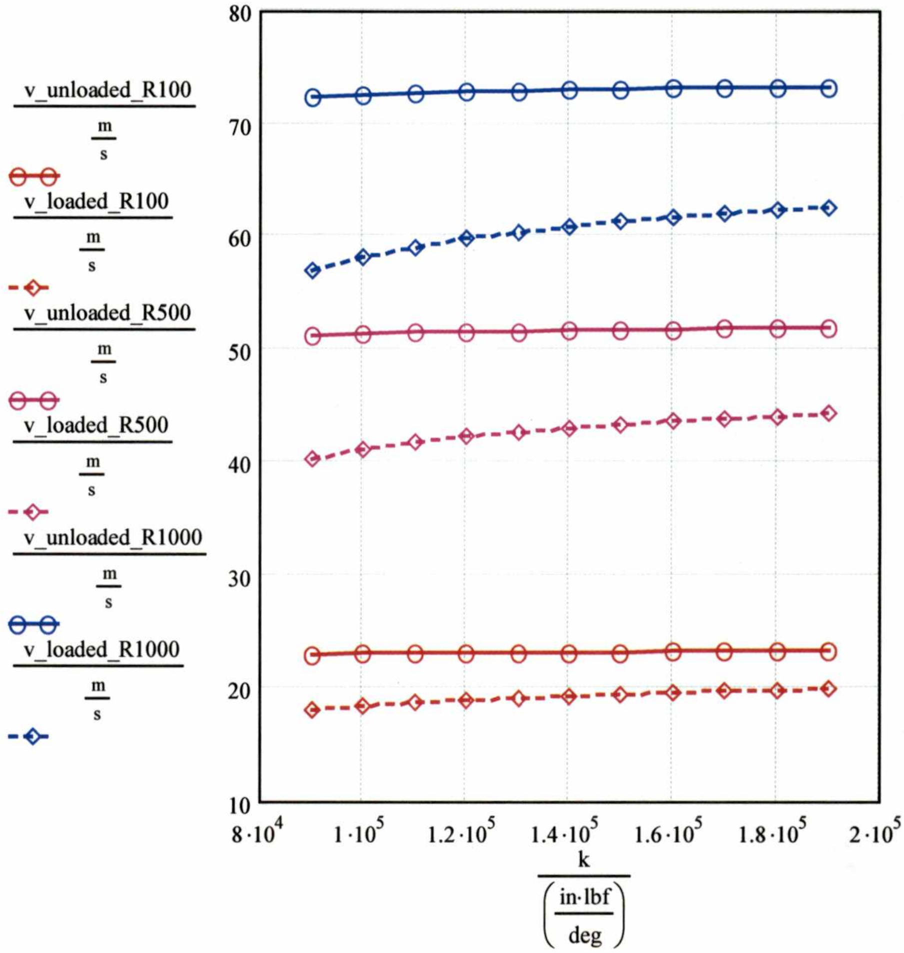

Fig 4.11 Liftoff Speed *v* Change With Roll Stiffness *k*

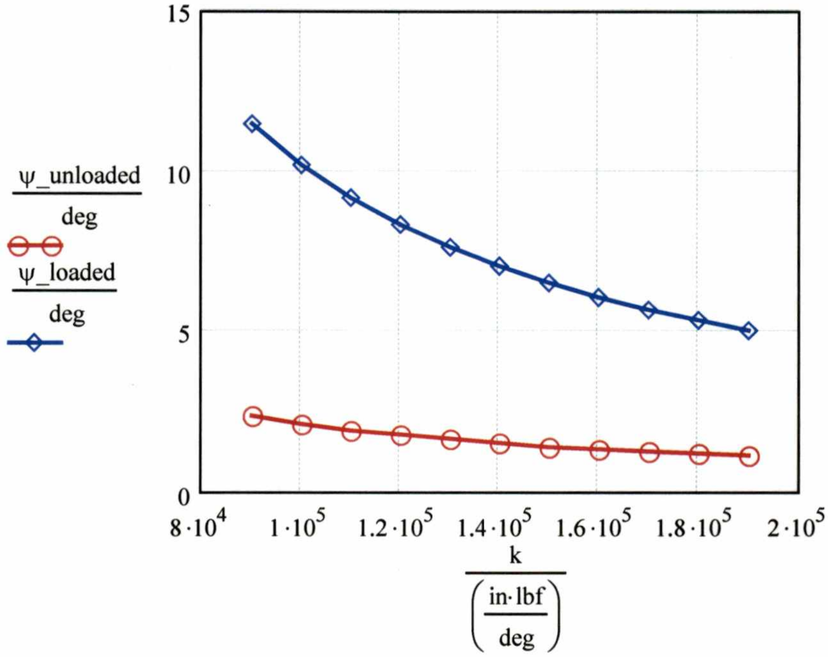

Fig 4.12 Liftoff Roll Angle ψ Change With Roll Stiffness k

From Fig 4.12, we find that with higher roll stiffness, the liftoff roll angle decreases for both loaded and unloaded trailer. (This is what intuition would lead us to expect. A stiffer spring produces a given restoring moment with less roll.) For a trailer rotating around a 500-meter radius circle, changing roll stiffness from 9,0000 in·lbf/deg to 19,0000 in·lbf/deg changes liftoff roll angle from 2.37° to 1.11° for an unloaded trailer and from 11.46° to 5.04° for a loaded trailer. Again the influence of roll stiffness for the loaded trailer is larger than that for the unloaded trailer.

The results above imply that higher roll stiffness of the trailer suspension results in better liftoff speed, and thus improves the liftoff and roll stability. The influence is more significant when the trailer is loaded.

4.1.3 Influence Of Cargo And Cargo Box Mass Distribution

4.1.3.1 Influence Of Center Of Gravity Height *h*

Cargo box center of gravity height h is another basic vehicle property that affects basic roll stability.

From Fig 4.13 and Fig 4.14, when h increases, the liftoff speed becomes lower and the roll angle becomes slightly higher. When the trailer rotates around a circle with radius of 500 meters, changing the center of gravity height from 12 in to 32 in changes the liftoff speed from 57.09 m/s to 47.35 m/s for an unloaded trailer and from 49.52 m/s to 37.71 m/s for a loaded trailer. The influence of the center of gravity height change is almost the same for both loaded and unloaded trailers. For both cases, the magnitude of the change in liftoff speed is quite significant.

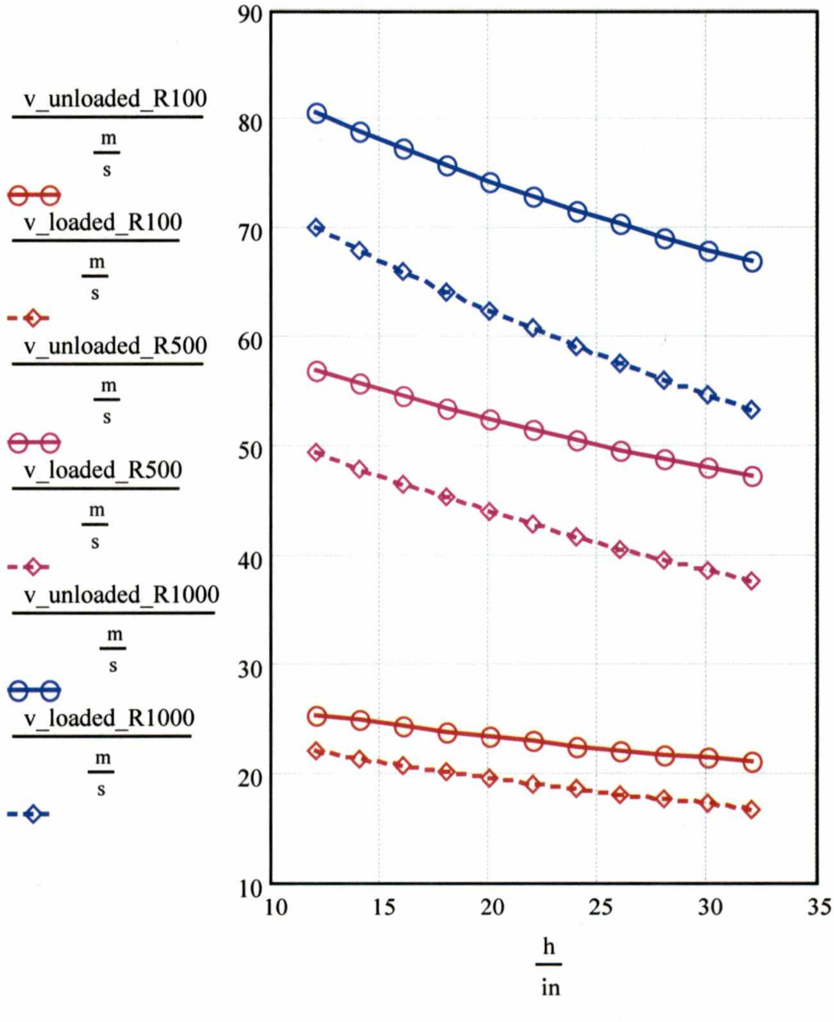

Fig 4.13 Liftoff Speed *v* Change With Cargo Box Center Of Gravity Height *h*

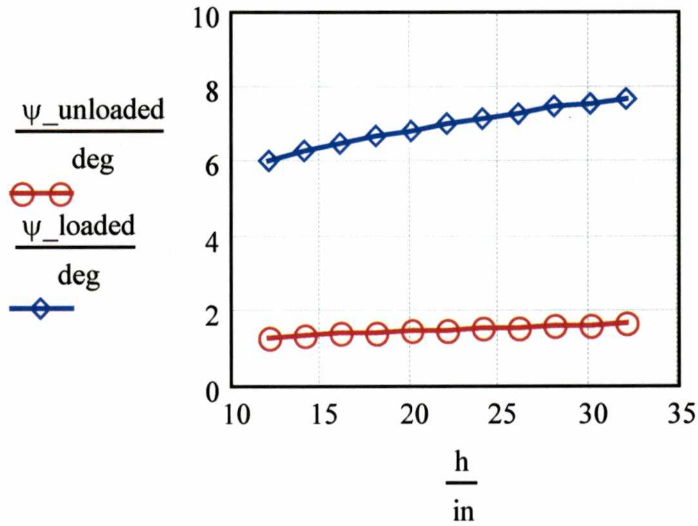

Fig 4.14 Liftoff Roll Angle ψ Change With Cargo Box Center Of Gravity Height h

From Fig 4.14, we find that with higher center of gravity height, the liftoff roll angle increases for both loaded and unloaded trailers. When the center of gravity height changes from 12 in to 32 in for a trailer rotating around a 500-meter radius circle, the liftoff roll angle changes from 1.29° to 1.66° for the unloaded trailer and from 6.04° to 7.68° for the loaded trailer.

Because the *h* change affects the liftoff property significantly, especially for loaded trailer, lowering the center of gravity position will significantly increase roll stability.

4.1.3.2 Influence Of Cargo Box Center Of Gravity Fore-Aft Location *a*

From Fig 4.15 and Fig 4.16, when *a* increases, or when the cargo is nearer from the trailer axle, both the liftoff speed and the liftoff roll angle increase, which means liftoff will be less likely. When center of gravity fore-aft location changes from 143 in to 343 in for a trailer rotating around a circle with radius of 500 meters, the change in liftoff speed is from 48.50 m/s to 52.16 m/s for an unloaded trailer and from 37.15 m/s to 43.81 m/s for a loaded trailer.

From Fig 4.16, we find that with a larger *a* value, the liftoff roll angle increases for both loaded and unloaded trailers. When center of gravity fore-aft location changes from 143 in to 343 in for a trailer rotating around a 500-meter radius circle, the liftoff roll angle changes from 1.07° to 1.62° for an unloaded trailer and from 4.02° to 7.75° for a loaded trailer.

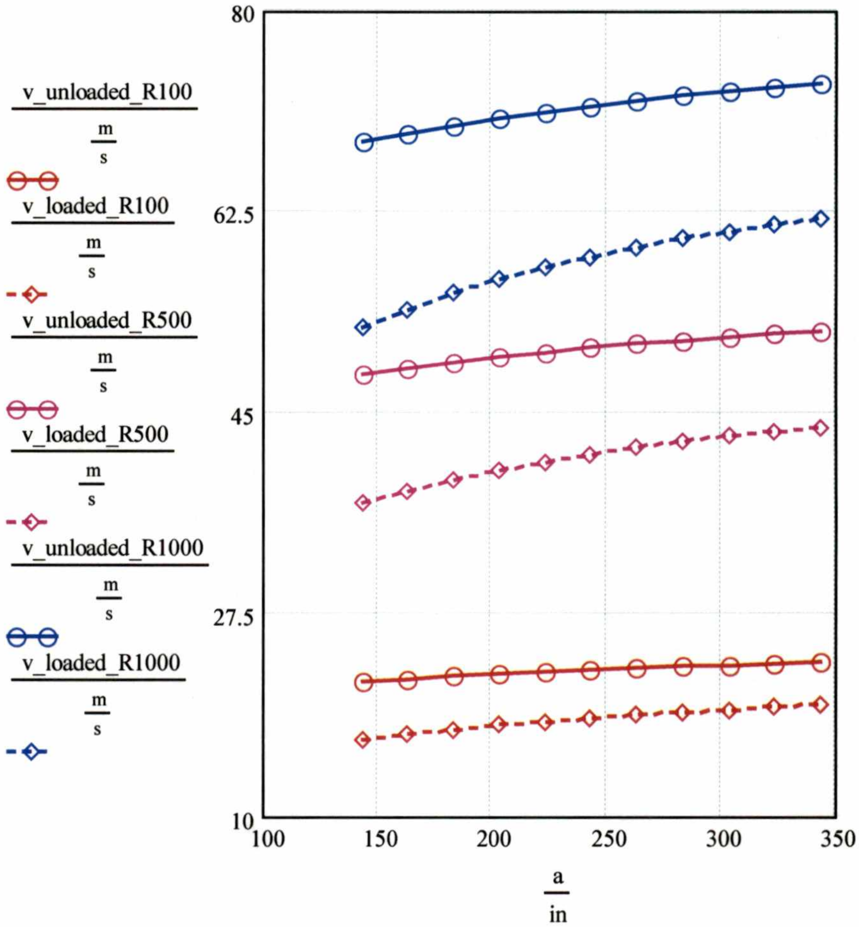

Fig 4.15 Liftoff Speed *v* Change With Longitudinal Center Of Gravity Position *a*

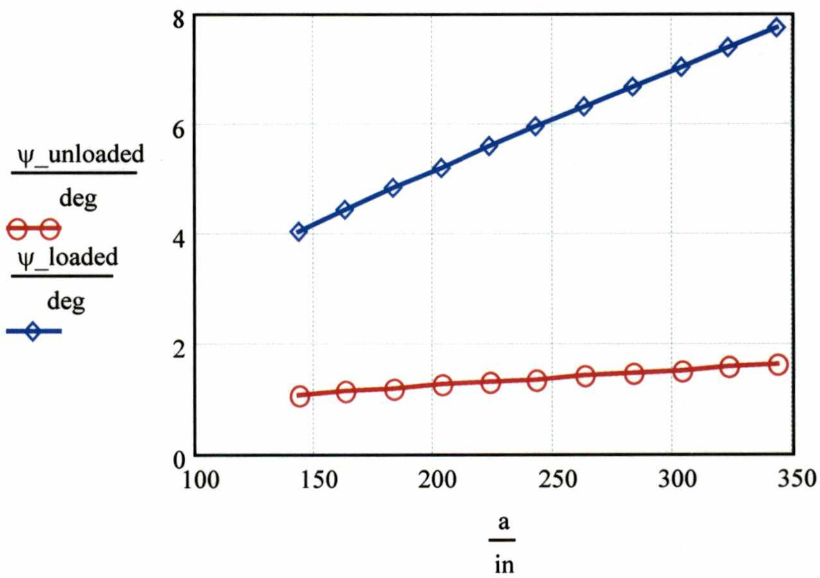

Fig4.16 Liftoff Roll Angle ψ Change With Longitudinal Center Of Gravity Position a

The result above implies that if the cargo is not large enough to fill the cargo box, it should be fastened to the rear of the cargo box (to be nearer from the stiffest suspension) to improve the liftoff and roll stability.

Notice that the liftoff velocity curves are flat even when the change of a is large. We conclude that the influence of a on the liftoff speed is relatively small. Notice also that when the trailer is loaded, the curves are less flat, especially the roll angle curve.

4.1.3.3 Influence Of Center Of Gravity Lateral Location *t*

From Fig 4.17 and Fig 4.18, when t becomes more positive, or the center of gravity moves away from the roll direction, the liftoff velocity increases sharply but the liftoff roll angle decreases. If t becomes more negative, or the center of gravity moves towards the roll direction, the liftoff velocity decreases and the roll angle increases.

The change of t affects the liftoff properties quite strongly. When t changes between –10 and 10 inches, the liftoff speed for a loaded trailer on a 500-meter radius circle changes from 29.59 m/s to 52.84 m/s, which is a 78.6% change. The change for an unloaded trailer in the same turning circle is from 42.51 m/s to 59.31 m/s, which is a 39.5% change. Liftoff roll angle changes for the same turning circle radius are from 8.55° to 5.5° for a loaded trailer (35.7% change) and from 1.82° to 1.20° (34% change) for an unloaded trailer.

The liftoff speed increases when the center of gravity moves towards the path center. But in practice, the path center can be at either side of the trailer. Hence, liftoff speed decreases sharply (for either a right or left turn) when there is any lateral offset of

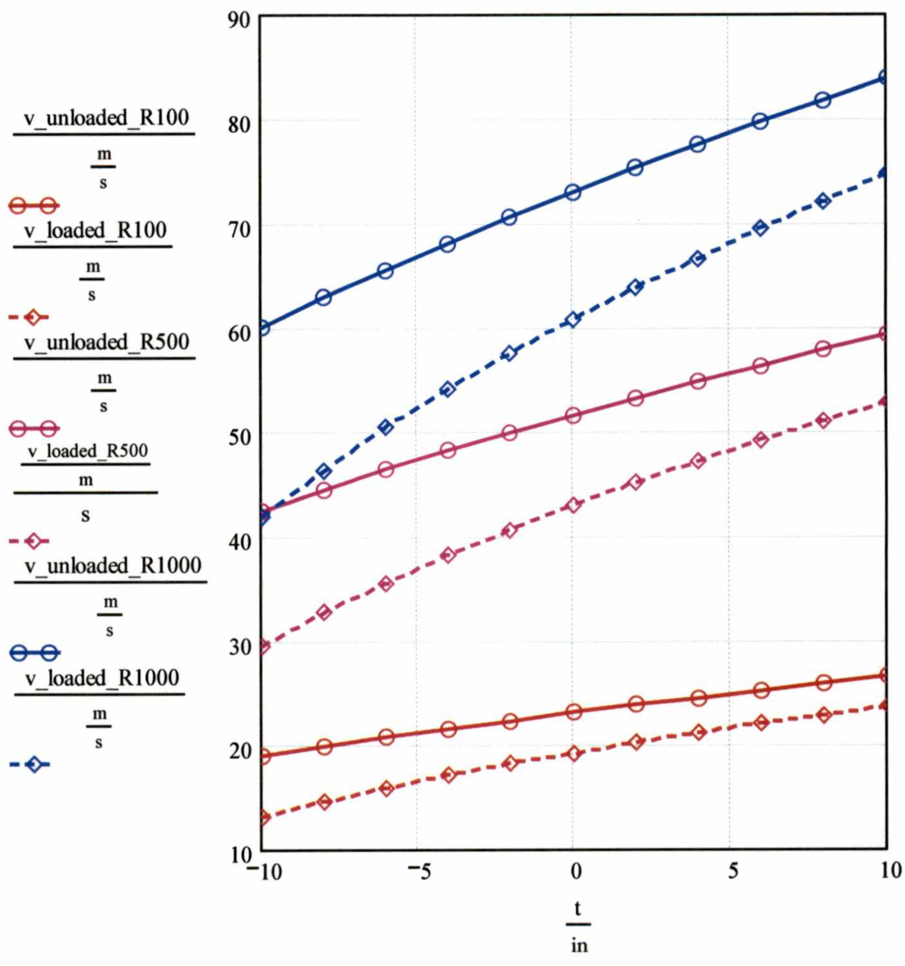

Fig 4.17 Liftoff Speed v Change With Lateral Center Of Gravity Position t

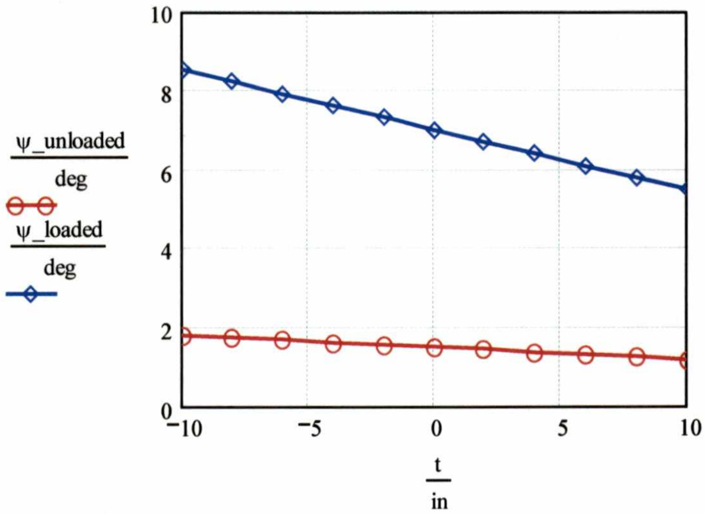

Fig 4.18 Liftoff Roll Angle ψ Change With Lateral Center Of Gravity Position t

the cargo, especially when the trailer is loaded. Considering the strong influence of the lateral center of gravity position on liftoff properties, we conclude that the mass center of the cargo should be positioned along the roll centerline.

4.1.4 The Importance Of Pertinent Mechanical Properties Of Trailer On Liftoff Performance

From the above results we can list the relative importance of different trailer properties on liftoff performance, as in Table 4.1.

Table 4.1 The Importance Of Pertinent Mechanical Properties On Liftoff Properties

Mechanical Properties	Importance on liftoff properties
Weight	High
Path radius	High
Track width	High
Roll center height	Moderate
Roll stiffness	Moderate
Fifth wheel height	Low
Center of gravity height	High
Fore-aft center of gravity location	Low
Lateral center of gravity location	High

4.2 Verification Of The Theory

There are several ways in which one might verify the validity of the liftoff model discussed above. These include comparison with experimental data, comparison with another computer-based model, and comparison with another theoretical derivation. Comparison with experimental data is not yet possible, because no suitable data has been published and generation of new data is beyond the scope of this thesis. It is recommended as an area for future work. Comparison with a simulation is possible in principle, but is beyond the scope of this work. It is also recommended as an area for future work. The third method of verification is discussed below. The equations presented above and the numerical results are compared with an analysis and computations based on Lagrange's equations of motion.

4.2.1 Lagrange's Equations For Trailers In Plane Circular Steady State Turning

Lagrange's equations of motion are then expressed as

$$(4.1)\qquad \frac{d}{dt}\left(\frac{\partial T}{\partial \dot{q}_j}\right)-\frac{\partial T}{\partial q_j}+\frac{\partial V}{\partial q_j}=Q_j,\ j=1,2,\ldots,M\,.$$

If we consider only roll of the cargo box and the rotation of the trailer associated with moving along a circular path, the trailer has two degrees of freedom. In the equations, the two generalized coordinates can be defined as the roll angle of the cargo box $q_1=\psi$ and the angular displacement of the trailer $q_2=\phi$ around path center O, i.e.

$$\bar{q}=\begin{Bmatrix}\psi\\ \phi\end{Bmatrix}.$$

In plane circular steady state turning, trailer angular speed $\dot{\phi}$ is a constant and $\dot{\phi} = \omega = \dfrac{v}{R}$. Also, the roll angular speed is $\dot{\psi} = 0$, because ψ is a constant when the path radius R and speed v are fixed.

In steady state turning, only conservative forces are needed to maintain the steady state. So the virtual work done by generalized forces $\delta W = 0$. (Frictional dissipation associated with sideslip of the trailer's tires is exactly balanced by energy delivered to the trailer by forces at the fifth wheel.) Thus generalized forces $Q_j = 0$ in Lagrange's equations. Since none of the kinetic energy and the potential energy contains ϕ, Lagrange's equations then become

$$(4.2) \qquad -\frac{\partial T}{\partial \psi} + \frac{\partial V}{\partial \psi} = 0,$$

$$(4.3) \qquad \frac{d}{dt}\left(\frac{\partial T}{\partial \dot{\phi}}\right) = 0.$$

Equation (4.3) is just a statement of conservation of angular momentum. It implies that

$$\frac{\partial T}{\partial \dot{\phi}} = constant.$$

But without knowing linear speed v and roll angle ψ, we do not know what the constant is.

Equation (4.2) is an "equilibrium" statement. It gives a relationship between v, R and ψ and is just what we want to verify the equations obtained previously from Newtonian kinetics in chapter 3.

In (4.2), the kinetic energy of the system is the sum of the kinetic energies of the undercarriage and the cargo box,

$$(4.4) \qquad T = T_C + T_Q .$$

But the kinetic energy of the undercarriage is

$$T_Q = \frac{1}{2} m_Q \bar{v}_Q \cdot \bar{v}_Q + \frac{1}{2} \bar{\omega} \cdot I_Q \cdot \bar{\omega} ,$$

in which

$$\bar{v}_Q = \bar{\omega} \times \bar{r}_{OQ} .$$

From chapter 3 we know that none of $\bar{\omega}$, $\bar{r}_{OQ}$ and I_Q depend on ψ, so that

$$(4.5) \qquad \frac{\partial T_Q}{\partial \psi} = 0 .$$

From (4.2), (4.3) and (4.4), we then have

$$(4.6) \qquad -\frac{\partial T_C}{\partial \psi} + \frac{\partial V}{\partial \psi} = 0 ,$$

which is the Lagrange's equation for trailer steady turning.

In equation (4.6),

$$(4.7) \qquad T_C = \frac{1}{2} m_C \bar{v}_C \cdot \bar{v}_C + \frac{1}{2} \bar{\omega} \cdot I_C \cdot \bar{\omega} ,$$

in which

$$(4.8) \qquad \bar{v}_C = \bar{\omega} \times \bar{r}_{OC} .$$

From chapter 3 we know that $\bar{\omega} = \frac{v}{R} \cdot \bar{u}_3$ and that it does not depend on ψ. But $\bar{r}_{OC}$ and I_C are both functions of ψ when they are expressed in a reference frame that does not roll with the trailer.

From chapter 3 we know that

$$\bar{r}_{OC} = \bar{r}_{OA} + R_{U-u}{}^{T} \cdot \bar{r}_{AC}^{0} ,$$

in which

$$R_{U-u} = R_{u2}^T(-(90-\delta)) \cdot R_{u1}(\psi) \cdot R_{u2}(-(90-\delta))$$

and

$$I_C = R_{U-u}{}^T \cdot I_C^0 \cdot R_{U-u}.$$

Then the derivative of kinetic energy is

$$\begin{aligned}
&\frac{\partial T_C}{\partial \psi} = m_C \cdot \overline{\omega} \times [R_{u2}^T(-(90-\delta)) \cdot \frac{\partial (R_{u1}(-\psi))}{\partial \psi} \cdot R_{u2}(-(90-\delta)) \cdot \overline{r}_{AC}^0] \cdot \overline{v}_C \\
(4.9) \quad &+ \frac{1}{2} \cdot \overline{\omega} \cdot R_{u2}(90-\delta)[\frac{\partial (R_{u1}(-\psi))}{\partial \psi} \cdot R_{u2}(-(90-\delta)) \cdot I_C^0 \cdot R_{u2}(90-\delta) \cdot R_{u1}(\psi) \\
&+ R_{u1}(-\psi) \cdot R_{u2}(-(90-\delta)) \cdot I_C^0 \cdot R_{u2}(90-\delta) \cdot \frac{\partial (R_{u1}(\psi))}{\partial \psi}] R_{u2}{}^T(90-\delta) \cdot \overline{\omega}.
\end{aligned}$$

On the other hand, the potential energy function of the trailer is

$$V = W_C(\overline{r}_{OC} \cdot \overline{u}_3) + \frac{1}{2} k_0 \psi^2.$$

The derivative of the potential energy expression is

$$(4.10) \quad \frac{\partial V}{\partial \psi} = W_C[R_{u2}^T(-(90-\delta)) \cdot \frac{\partial (R_{u1}(-\psi))}{\partial \psi} \cdot R_{u2}(-(90-\delta)) \cdot \overline{r}_{AC}^0] \cdot \overline{u}_3 + k_0 \psi.$$

From (4.6), (4.9) and (4.10), we get the Lagrange's equation for trailer liftoff in the steady turning maneuver,

$$\begin{aligned}
&-\{m_C \cdot \overline{\omega} \times [R_{u2}^T(-(90-\delta)) \cdot \frac{\partial (R_{u1}(-\psi))}{\partial \psi} \cdot R_{u2}(-(90-\delta)) \cdot \overline{r}_{AC}^0] \cdot \overline{v}_C \\
&+ \frac{1}{2} \cdot \overline{\omega} \cdot R_{u2}(90-\delta)[\frac{\partial (R_{u1}(-\psi))}{\partial \psi} \cdot R_{u2}(-(90-\delta)) \cdot I_C^0 \cdot R_{u2}(90-\delta) \cdot R_{u1}(\psi) \\
(4.11) \quad &+ R_{u1}(-\psi) \cdot R_{u2}(-(90-\delta)) \cdot I_C^0 \cdot R_{u2}(90-\delta) \cdot \frac{\partial (R_{u1}(\psi))}{\partial \psi}] R_{u2}^T(90-\delta) \cdot \overline{\omega} \\
&+ W_C[R_{u2}^T(-(90-\delta)) \cdot \frac{\partial (R_{u1}(-\psi))}{\partial \psi} \cdot R_{u2}(-(90-\delta)) \cdot \overline{r}_{AC}^0] \cdot \overline{u}_3 + k_0 \psi = 0.
\end{aligned}$$

4.2.2 Results from the Lagrange's equation

Since equation (4.11) indicates the relationship among v, R and ψ, to be compared with the results from equations (3.19) and (3.20), we have to provide two of the three unknowns to get the third one.

When R changes from 100 meters to 1000 meters and v is given from the solution of (3.19) and (3.20), we plot the ψ values calculated from (4.11) and from the (3.19), (3.20) system. The results are shown in Fig 4.19, and the difference between the two results is shown in Fig 4.20.

From Fig 4.20 we find that the difference between the liftoff roll angle from Lagrange's equations and that from the Newtonian method is just 0.089%.

From Fig 4.21 and Fig 4.22 we also find that when the center of gravity height h changes, given v from (3.19) and (3.20), results from Lagrange's equations are almost the same as that got from (3.19) and (3.20), the difference between the two methods being about 0.089%. We can safely say the results from the two methods are practically identical and that the theory in Chapter 3 is shown to be correct for the chosen model. The accuracy of the model in predicting real truck motion is yet to be established and would require further work of the kind described above in the first paragraph of section 4.2.

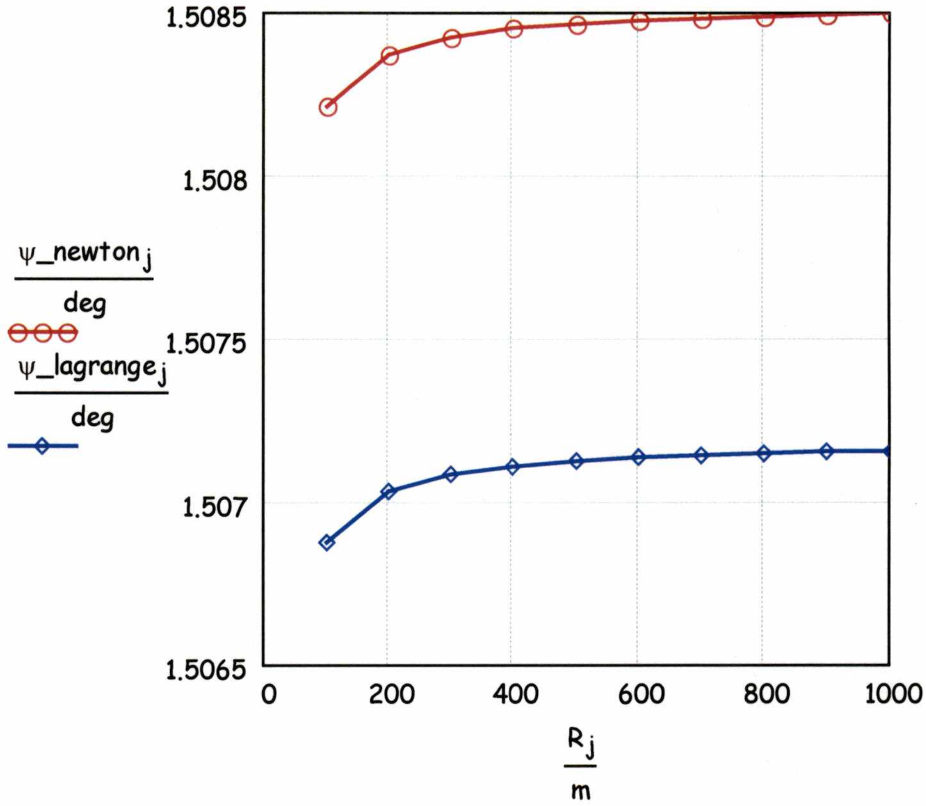

Fig 4.19 Liftoff Roll Angle ψ Calculated From Lagrange's Equation Given Liftoff Speed v And The Roll Angle Solved From Newton's Equations In Chapter 3

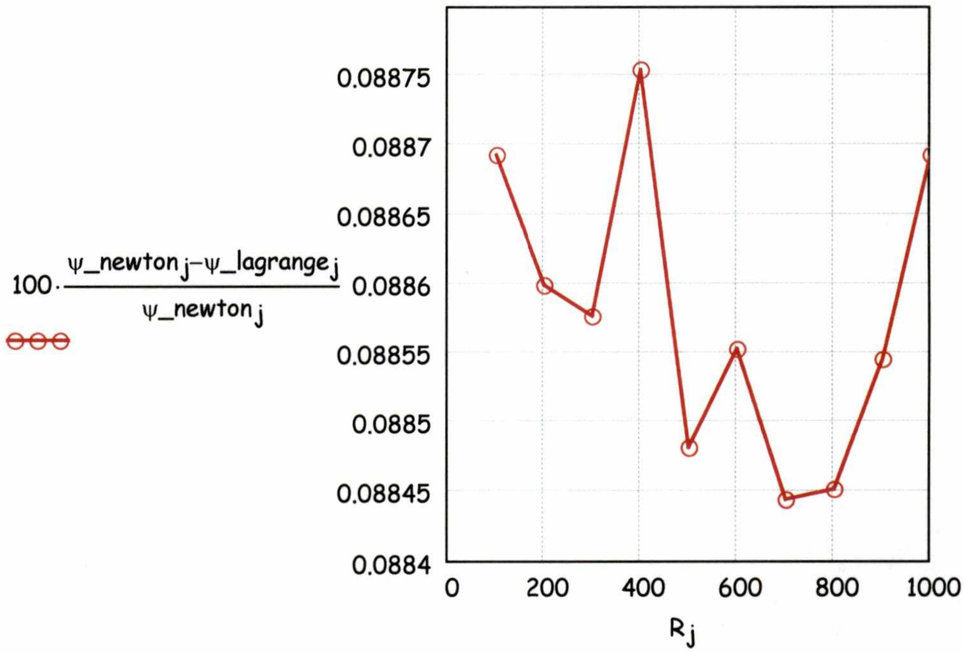

Fig 4.20 Difference Of Calculated Liftoff Roll Angle ψ From Lagrange's And From

Newton's Equations

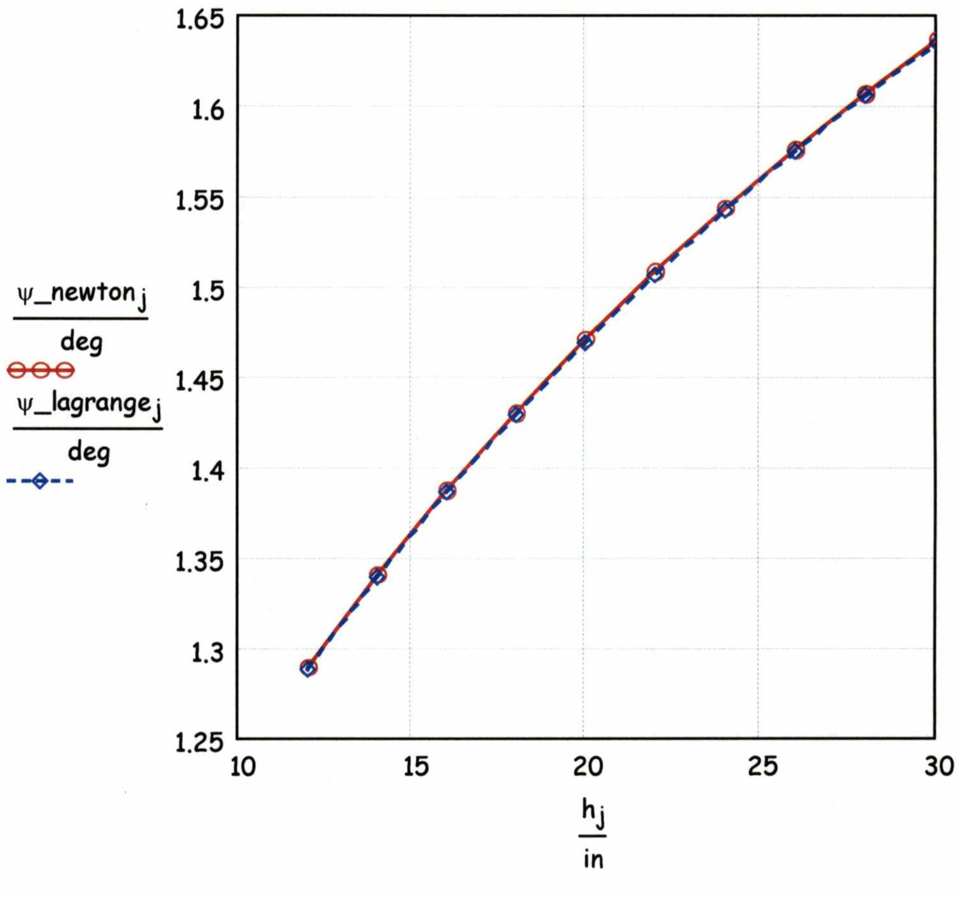

Fig 4.21 Liftoff Roll Angle ψ From Lagrange's And From Newton's Equations When Center Of Gravity Height h Changes

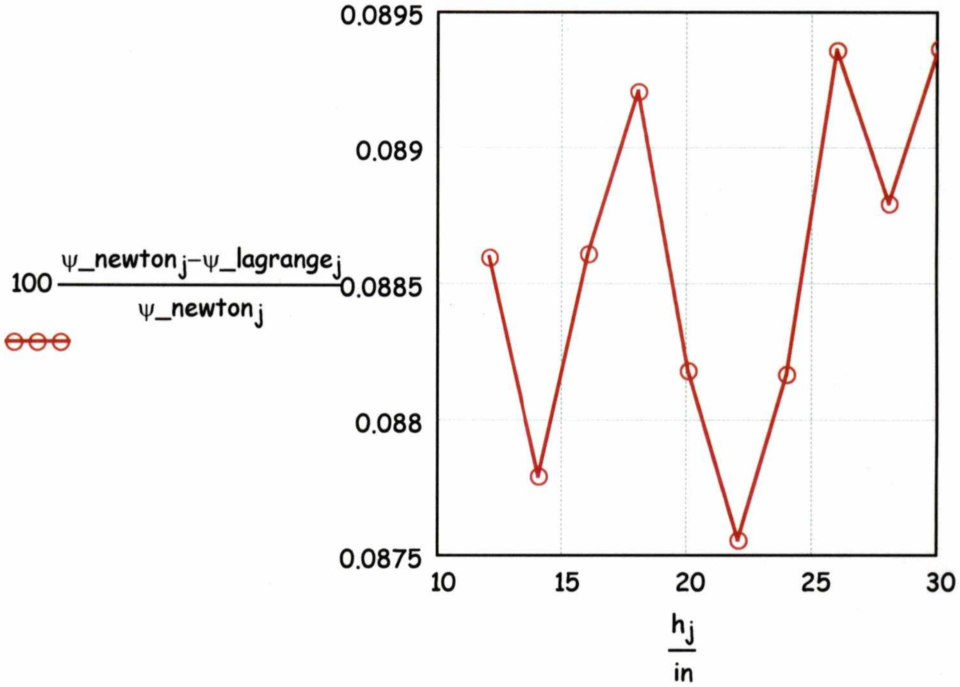

Fig 4.22 Difference Of Calculated Liftoff Roll Angle ψ From Lagrange's And From Newton's Equations When Center Of Gravity Height h Changes

Chapter 5

Use Of The Model — Trailer With One Hung Cargo In Steady Turning

In addition to evaluating the influence of fixed cargo in the cargo box, the model discussed above can also be used to evaluate the influence of moving cargo on the liftoff properties. In this chapter, a simple example of usage of the model is provided. A cargo hanging from the ceiling of the cargo box is considered, and its influence on the liftoff properties of the trailer is discussed.

5.1 Three Dimensional Trailer Model With One Hung Cargo

Consider the motion of the trailer and the cargo hung on the ceiling shown in Fig 5.1. Let the cargo be modeled as another rigid body with center of gravity at E.

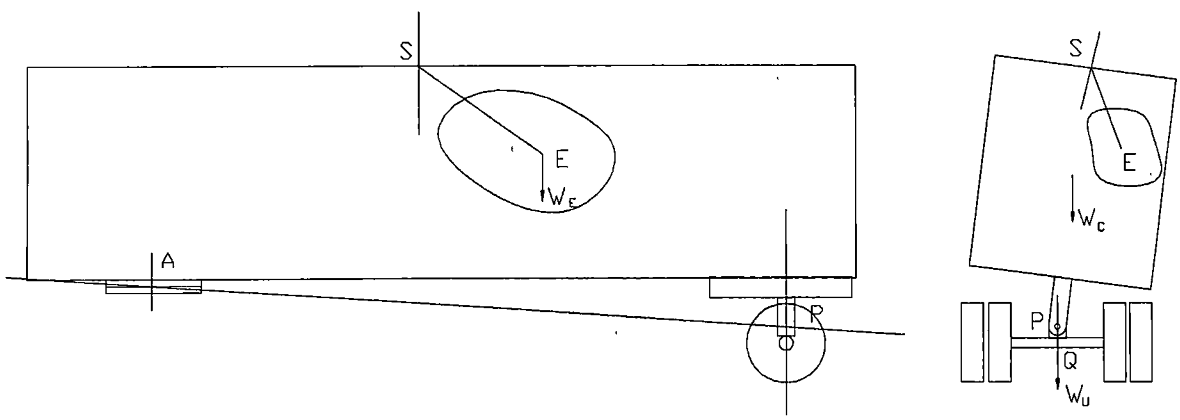

Fig. 5.1 Two Rigid Body Trailer With One Hanging Cargo Model

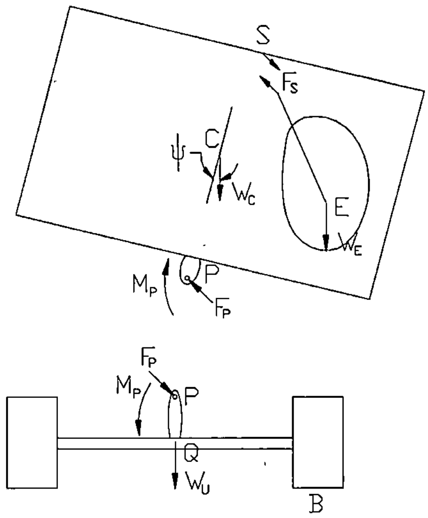

Fig. 5.2 Free Body Diagram For The Trailer And The Hanging Cargo

During turning, the forces and moments among the rigid bodies are shown in Fig 5.2.

Assume the link at point S is a sphere pivot, so that the torques at point S can be ignored. Similar to equation (3.1), moment summation about the fifth wheel A gives

(5.1) $$\Sigma \overline{M}_A = \overline{r}_{AP} \times \overline{F}_P + \overline{r}_{AS} \times \overline{F}_S + \overline{r}_{AC} \times \overline{W}_C - \overline{M}_P .$$

For the liftoff condition, moment summation about the contact line B still gives equation (3.2),

$$\Sigma \overline{M}_B = \overline{M}_P + \overline{r}_{BP} \times \left(-\overline{F}_P\right) + \overline{r}_{BQ} \times \overline{W}_U .$$

For the hung cargo, moment summation at center of gravity E is

(5.2) $$\Sigma \overline{M}_E = \overline{r}_{ES} \times (-\overline{F}_S) = \overline{r}_{SE} \times \overline{F}_S .$$

Force summation at E is

(5.3) $$\Sigma \overline{F}_E = m_E \cdot \overline{a}_E .$$

From Fig. 5.2, the force summation at E is also

$$(5.4) \qquad \Sigma\overline{F}_E = -\overline{F}_S + \overline{W}_E .$$

Thus from (5.3) and (5.4),

$$(5.5) \qquad \overline{F}_S = \overline{W}_E - m_E \cdot \overline{a}_E .$$

Substituting (5.5) into (5.2) gives

$$(5.6) \qquad \Sigma\overline{M}_E = \overline{r}_{SE} \times (\overline{W}_E - m_E \cdot \overline{a}_E) .$$

If we add (5.1) and (5.2) and take the dot product of $\overline{r}_{AB}$ with both sides of the equation, we eliminate the force and moment at P. Substituting (5.5) into the summation then gives

$$(5.7) \qquad (\Sigma\overline{M}_A + \Sigma\overline{M}_B)\cdot\overline{r}_{AB} = [\overline{r}_{AC} \times \overline{W}_C + \overline{r}_{BQ} \times \overline{W}_U + \overline{r}_{AS} \times (\overline{W}_E - m_E \cdot \overline{a}_E)] \cdot \overline{r}_{AB} .$$

In this equation,

$$(5.8) \qquad \overline{a}_E = \overline{a}_S + \overline{a}_{E/S} ,$$

in which

$$\overline{a}_S = \overline{a}_C + \overline{\alpha}_C \times \overline{r}_{CS} + \overline{\omega}_C \times (\overline{\omega}_C \times \overline{r}_{CS}),$$

and

$$\overline{a}_{E/S} = \overline{\alpha}_E \times \overline{r}_{SE} + \overline{\omega}_E \times (\overline{\omega}_E \times \overline{r}_{SE}).$$

Consider also (3.8)

$$\overline{a}_C = \overline{\alpha}_C \times \overline{r}_{OC} + \overline{\omega}_C \times (\overline{\omega}_C \times \overline{r}_{OC}),$$

Then $\overline{a}_S$ can be written as

$$\overline{a}_S = \overline{\alpha}_C \times \overline{r}_{OS} + \overline{\omega}_C \times (\overline{\omega}_C \times \overline{r}_{OS}),$$

in which

$$\bar{r}_{OS} = \bar{r}_{OC} + \bar{r}_{CS}.$$

Considering (3.4) through (3.10) and (5.8), we find that (5.7) becomes

$$\begin{aligned}(5.9)\qquad & \bar{r}_{AB} \cdot \{\dot{I}_C \cdot \bar{\omega}_C + I_C \cdot \bar{\alpha}_C + \bar{\omega}_C \times (I_C \cdot \bar{\omega}_C) + I_Q \cdot \bar{\alpha} + \bar{\omega} \times (I_Q \cdot \bar{\omega}) + \dot{I}_Q \cdot \bar{\omega} \\ & + \bar{r}_{AC} \times m_C[\bar{\alpha}_C \times \bar{r}_{OC} + \bar{\omega}_C \times (\bar{\omega}_C \times \bar{r}_{OC}) - \bar{g}] + \bar{r}_{BQ} \times m_U[\bar{\alpha} \times \bar{r}_{OQ} \\ & + \bar{\omega} \times (\bar{\omega} \times \bar{r}_{OQ}) - \bar{g}] + \bar{r}_{AS} \times m_E[\bar{\alpha}_C \times \bar{r}_{OS} + \bar{\omega}_C \times (\bar{\omega}_C \times \bar{r}_{OS}) + \bar{\alpha}_E \times \bar{r}_{SE} \\ & + \bar{\omega}_E \times (\bar{\omega}_E \times \bar{r}_{SE}) - \bar{g}]\} = 0.\end{aligned}$$

This is the first motion equation for a trailer in arbitrary motion with one cargo hung on the ceiling.

If we consider the roll stiffness of the suspension as in chapter three, and take the dot product of both sides with $\bar{r}_{AP}$, equation (5.1) can be written as

$$\begin{aligned}(5.10)\qquad & \bar{r}_{AP} \cdot \{\dot{I}_C \cdot \bar{\omega}_C + I_C \cdot \bar{\alpha}_C + \bar{\omega}_C \times (I_C \cdot \bar{\omega}_C) + \bar{r}_{AC} \times m_C[\bar{\alpha}_C \times \bar{r}_{OC} \\ & + \bar{\omega}_C \times (\bar{\omega}_C \times \bar{r}_{OC}) - \bar{g}] + \bar{r}_{AS} \times m_E[\bar{\alpha}_C \times \bar{r}_{OS} + \bar{\omega}_C \times (\bar{\omega}_C \times \bar{r}_{OS}) \\ & + \bar{\alpha}_E \times \bar{r}_{SE} + \bar{\omega}_E \times (\bar{\omega}_E \times \bar{r}_{SE}) - \bar{g}] + \bar{k} \cdot \psi\} = 0.\end{aligned}$$

This is the second motion equation for a cargo box in arbitrary motion with one hung cargo.

From rigid body dynamics,

$$(5.11)\qquad \Sigma \bar{M}_E = \dot{\bar{H}}_E = \dot{I}_E \cdot \omega_E + I_E \cdot \bar{\alpha}_E + \bar{\omega}_E \times (I_E \cdot \bar{\omega}_E).$$

Substituting (5.11) into (5.6) gives

$$\begin{aligned}(5.12)\qquad & \dot{I}_E \cdot \omega_E + I_E \cdot \bar{\alpha}_E + \bar{\omega}_E \times (I_E \cdot \bar{\omega}_E) + \bar{r}_{SE} \times m_E[\bar{\alpha}_C \times \bar{r}_{OS} + \bar{\omega}_C \times (\bar{\omega}_C \times \bar{r}_{OS}) \\ & + \bar{\alpha}_E \times \bar{r}_{SE} + \bar{\omega}_E \times (\bar{\omega}_E \times \bar{r}_{SE}) - \bar{g}] = 0,\end{aligned}$$

This is the motion equation for the hung cargo in a trailer executing arbitrary motion.

In steady turning with constant velocity, the relationships between the angular velocity and angular acceleration of the cargo box and the hung cargo can be expressed as

$$\overline{\omega}_E = \overline{\omega}_C + \overline{\Omega}_{E/C}\,,\ \overline{\alpha}_E = \overline{\alpha}_C + \dot{\overline{\Omega}}_{E/C}\,,$$

and

$$\overline{\Omega} = 0\ ,\ \overline{\Omega}_{E/C} = 0\,,$$

$$\dot{\overline{\Omega}} = 0\,,\ \dot{\overline{\Omega}}_{E/C} = 0\,.$$

The angular acceleration of the undercarriage relative to inertial reference frame is, $\overline{\alpha} = 0$. And the time derivative of the inertia tensor at E is $\dot{I}_E = 0$.

Also, in steady turning,

$$\text{(5.13)}\qquad \Sigma\overline{M}_E = \dot{\overline{H}}_E = 0\,.$$

Then the angular velocity and angular acceleration become

$$\text{(5.14)}\qquad \overline{\omega}_E = \overline{\omega}_C = \overline{\omega}\,,\ \overline{\alpha}_E = \overline{\alpha}_C = \overline{\alpha} = 0\,.$$

Taking (5.13) and (5.14) into (5.9), (5.10) and (5.12) gives

$$\text{(5.15)}\qquad \begin{aligned}&\overline{r}_{AB}\cdot\{\overline{\omega}\times[(I_Q+I_C)\cdot\overline{\omega}]+\overline{r}_{AC}\times m_C[\overline{\omega}\times(\overline{\omega}\times\overline{r}_{OC})-\overline{g}]\\ &+\overline{r}_{BQ}\times m_U[\overline{\omega}\times(\overline{\omega}\times\overline{r}_{OQ})-\overline{g}]+\overline{r}_{AS}\times m_E[\overline{\omega}\times(\overline{\omega}\times\overline{r}_{OE})-\overline{g}]\}=0.\end{aligned}$$

$$\text{(5.16)}\qquad \begin{aligned}&\overline{r}_{AP}\cdot\{\overline{\omega}\times(I_C\cdot\overline{\omega})+\overline{r}_{AC}\times m_C[\overline{\omega}\times(\overline{\omega}\times\overline{r}_{OC})-\overline{g}]\\ &+\overline{r}_{AS}\times m_E[\overline{\omega}\times(\overline{\omega}\times\overline{r}_{OE})-\overline{g}]+\overline{k}\cdot\psi\}=0.\end{aligned}$$

$$\text{(5.17)}\qquad \overline{r}_{SE}\times m_E[\overline{\omega}\times(\overline{\omega}\times\overline{r}_{OE})-\overline{g}]=0\,.$$

These three equations are the three-dimensional model for liftoff of a trailer with one hung cargo in steady circular turning.

In plane circular turning in $(\overline{U}_1,\overline{U}_2,\overline{U}_3)$ system defined in chapter 3,

$$\overline{\omega} = \frac{v}{R} \cdot \overline{U}_3 .$$

In equation (5.15) and (5.16) in $(\overline{U}_1, \overline{U}_2, \overline{U}_3)$ system,

$$(5.18) \quad \overline{r}_{AS} = R_{U-u}{}^{T} \cdot \overline{r}_{AS}^{0}$$

in which

$$\overline{r}_{AS}^{0} = \begin{Bmatrix} -b \\ f \\ H \end{Bmatrix} \text{ is in body system } (\overline{u}_1, \overline{u}_2, \overline{u}_3),$$

and

$$R_{U-u} = R_{u2}^{T}(-(90-\delta)) \cdot R_{u1}(\psi) \cdot R_{u2}(-(90-\delta)).$$

We also have

$$(5.19) \quad \overline{r}_{OE} = \overline{r}_{OA} + \overline{r}_{AS} + \overline{r}_{SE} .$$

Define another body fixed coordinate system $(\overline{v}_1, \overline{v}_2, \overline{v}_3)$ that originates at point S and rolls with the cargo box as shown in Fig 5.3. The directions of the axes of this system are defined as

$\overline{v}_1$ = backward (directed from the front of the trailer toward the rear of the trailer),

$\overline{v}_2$ = port (left when facing forward),

$\overline{v}_3$ = down

From Fig 5.4, in the $(\overline{v}_1, \overline{v}_2, \overline{v}_3)$ system,

$$\overline{r}_{SE}^{v} = l \begin{Bmatrix} \cos(\phi)\cos(\theta) \\ -\cos(\phi)\sin(\theta) \\ \sin(\phi) \end{Bmatrix} .$$

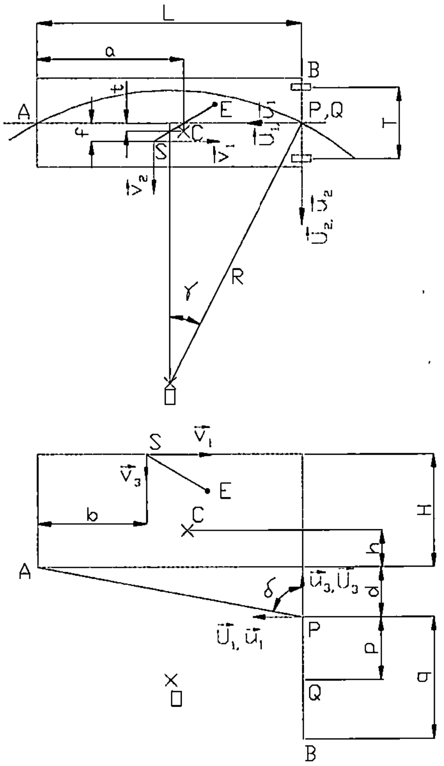

Fig. 5.3 Definition Of Lengths And Angles For The Trailer And Hanging Cargo

When it is transferred to the $(\overline{U}_1, \overline{U}_2, \overline{U}_3)$ system,

(5.20) $\quad \bar{r}_{SE} = R_{U\sim v}{}^{T} \cdot \bar{r}_{SE}^{\,v}$,

in which

$$R_{U\sim v} = R_{u2}(-(90+\delta)) \cdot R_{u1}(\psi) \cdot R_{u2}(-(90-\delta)),$$

and

$$R_{u2}(-(90+\delta)) = \begin{bmatrix} \cos(-(90+\delta)) & 0 & -\sin(-(90+\delta)) \\ 0 & 1 & 0 \\ \sin(-(90+\delta)) & 0 & \cos(-(90+\delta)) \end{bmatrix}.$$

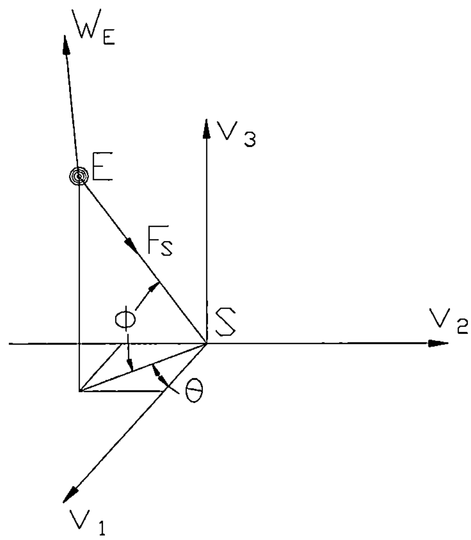

Fig. 5.4 Definition Of Angles In $(\overline{v}_1, \overline{v}_2, \overline{v}_3)$

Substituting equations (5.18) to (5.20) and (3.20) to (3.31) into equations (5.15) and (5.16), gives the liftoff equation for the trailer and the cargo box in plane circular steady turning in the $(\overline{U}_1, \overline{U}_2, \overline{U}_3)$ system.

Substituting equation (5.20) back into equation (5.17) gives the liftoff equation for the hung cargo in plane circular steady turning in the $(\overline{U}_1, \overline{U}_2, \overline{U}_3)$ system.

Unlike equations (5.15) and (5.16), equation (5.17) is a vector equation. But the three scalar components of (5.17) contain only two independent equations. These two, together with (5.15) and (5.16), form a system of four independent scalar equations. Solving this system gives the liftoff speed v, roll angle ψ, and the elevation and azimuthal angles ϕ and θ of the hung cargo.

5.2 Results

In this part, influence of the cargo on the liftoff properties will be investigated and discussed.

5.2.1 Influence Of Weight Of The Cargo

As discussed in chapter 4, the influence of the cargo weight is high. Fig 5.5 and Fig 5.6 show the liftoff properties of the trailer turning on a circle with 1000 meters radius.

From Fig 5.5 and Fig 5.6 we find that though the liftoff roll angle increases when the weight of the cargo increases, the vehicle speed to reach this roll angle decreases dramatically. When the hung cargo weight changes from 100 lbf to 1000 lbf, the liftoff speed changes from 51.02 m/s to 46.66 m/s, and the corresponding liftoff roll angle change is from 1.54° to 1.79°. So, heavier cargo makes liftoff more likely.

From Fig 5.7 and Fig 5.8, we can also find the movement of the hung cargo during steady turning. When the weight increases, the cargo's elevation decreases from 29.53° to 25.75° from its static position. But its backward moving increases from 0.22° to 0.23° from its static position. So, when the cargo becomes heavier, the hung cargo lifts less but moves backward more.

5.2.2 Influence of path radius *R*

In this section, the trailer with a 500-lbf cargo rotates steadily around different circles whose radii range from 100 m to 1000 m.

From Fig 5.9 and Fig 5.10, the influence of path radius *R* on the liftoff properties is found to be similar to what has been found in chapter 4. When the path radius changes

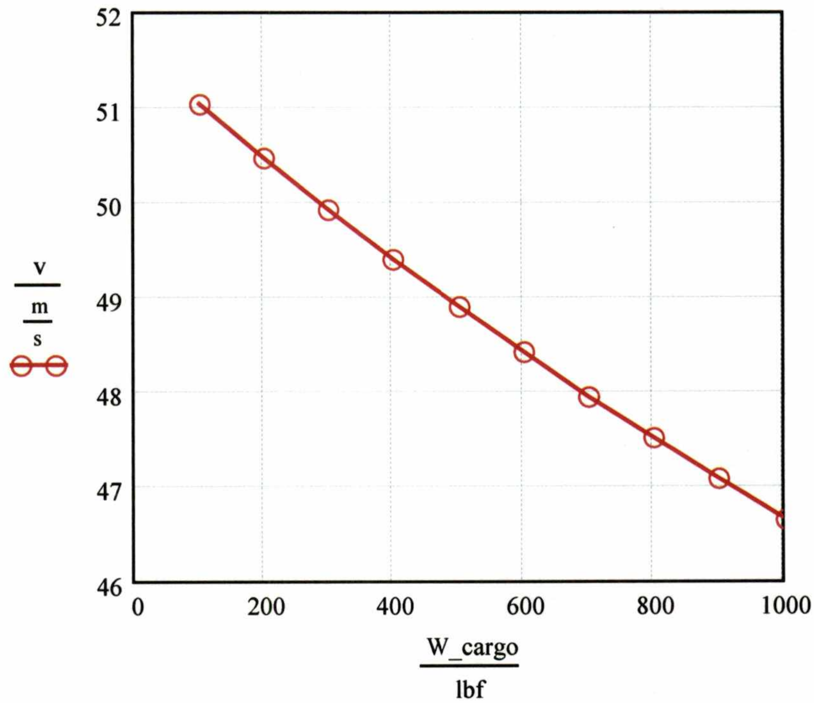

Fig 5.5 The Influence Of Cargo Weight W_E On Liftoff Speed v

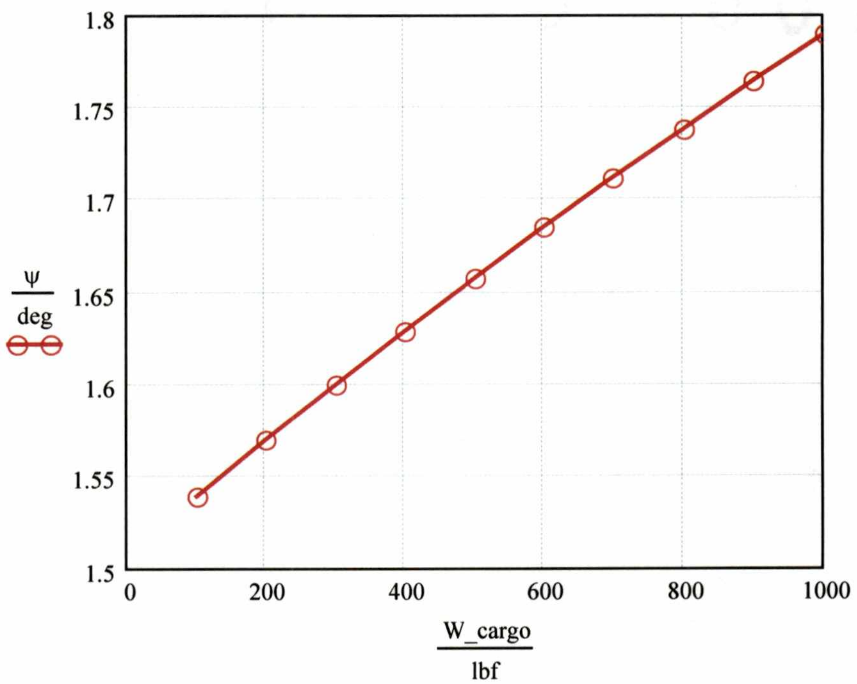

Fig 5.6 The Influence Of Cargo Weight W_E On Liftoff Roll Angle ψ

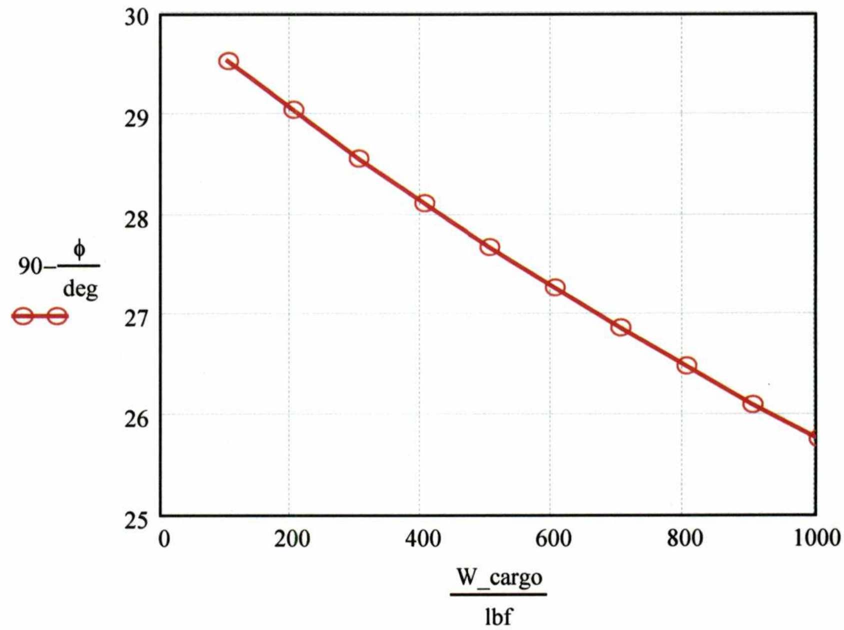

Fig 5.7 The Influence Of Cargo Weight W_E On Elevation Angle ϕ

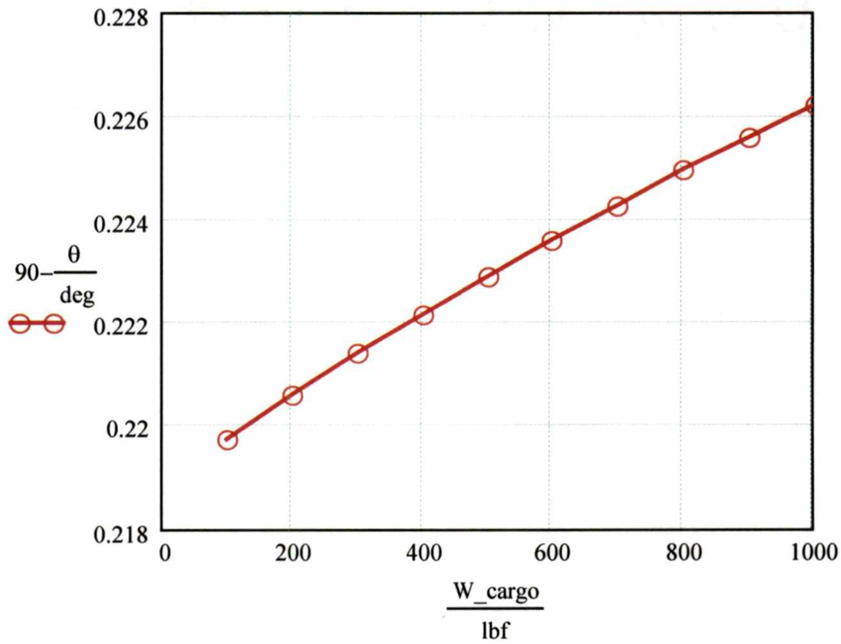

Fig 5.8 The Influence Of Cargo Weight W_E On Azimuthal Angle θ

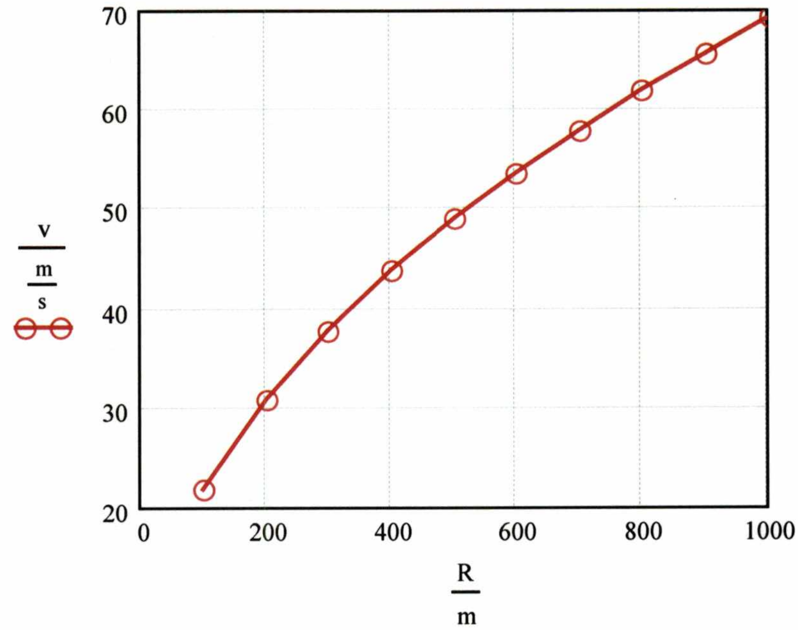

Fig 5.9 The Influence Of Path Radius *R* On Liftoff Speed *v*

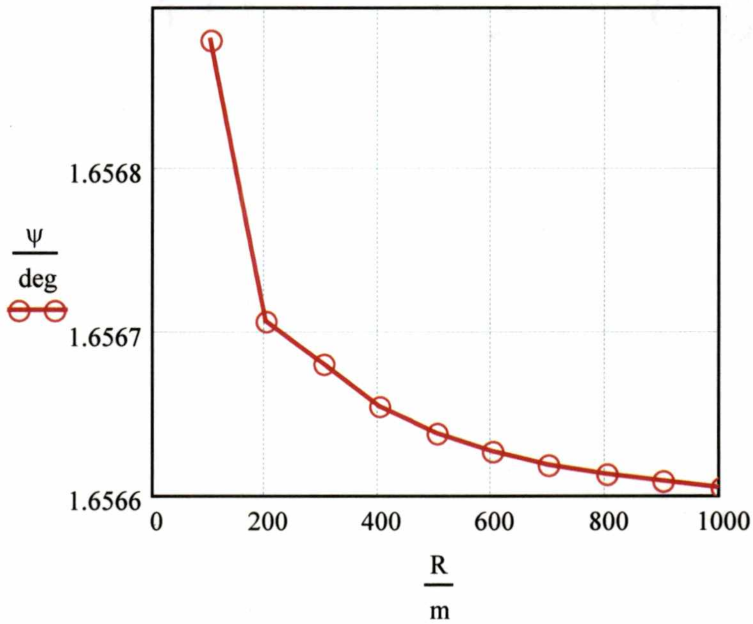

Fig 5.10 The Influence Of Path Radius R On Liftoff Roll Angle ψ

from 100 m to 1000 m, the change of the liftoff speed is from 21.88 m/s to 69.16 m/s. The change of the liftoff roll angle is from 1.6569° to 1.6566°, which makes the roll angle essentially unchanged.

From Fig 5.11 and Fig 5.12, the influence of path radius change on the lift and backward movement of the cargo can also be found. When the path radius increases, both the lift and the backward movement of the cargo become smaller. The change of elevation angle ϕ is from 27.76° to 27.67° and the change of θ is from 0.85° to 0.14° when path radius changes from 100m to 1000m. So, a larger circle makes the movement of the cargo smaller.

5.2.3 Influence of cargo box height *H*

From Fig 5.13 and Fig 5.14, we find that though the liftoff roll angle increases as the cargo box becomes higher, the liftoff speed decreases. When the cargo box height changes from 44 in to 244 in, the roll angle at liftoff increases from 1.58° to 1.72°, at the same time, the liftoff speed decreases from 50.86 m/s to 47.13 m/s when a 500-lbf cargo is hung on the ceiling of the cargo box. So, a taller cargo box makes liftoff more likely.

From Fig 4.15 and Fig 4.16, we can also find the effect on the movement of the hung cargo when the height of the cargo box height changes. From Fig 4.15 we find that the cargo lifts less when the cargo is higher. The elevation decreases from 29.42° to 26.11° when the cargo box height increases 200 in. The influence of the cargo box height on azimuthal angle is not very large. It changes only about 0.003°.

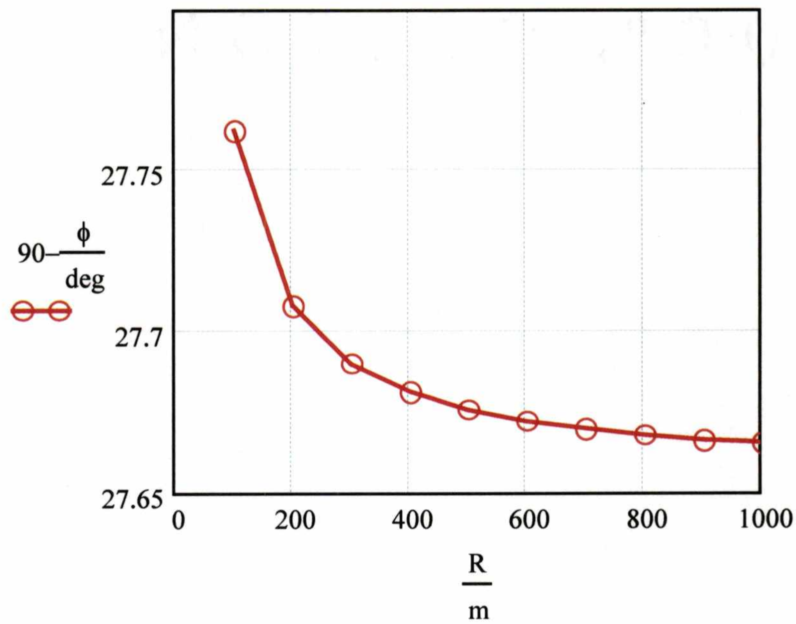

Fig 5.11 The Influence Of Path Radius R On Elevation Angle ϕ

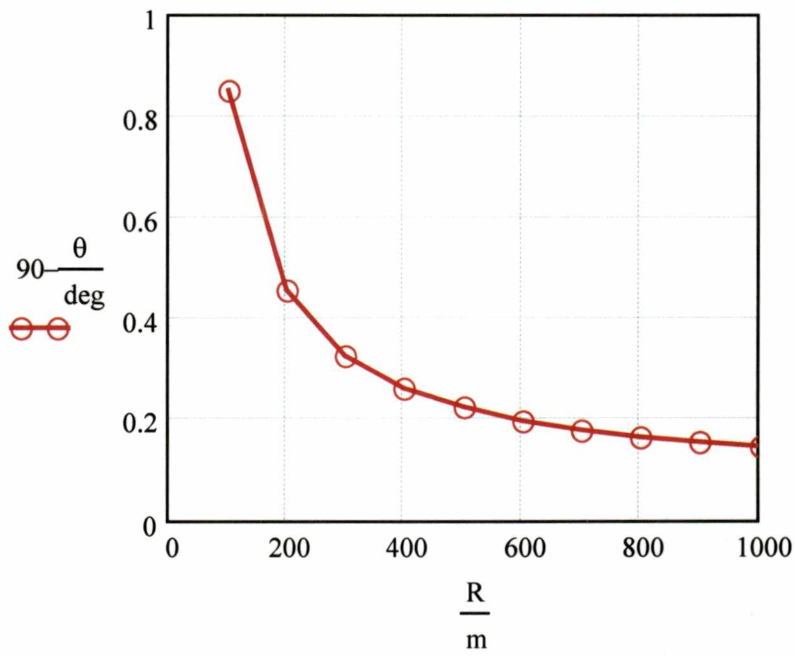

Fig 5.12 The Influence Of Path Radius R On Azimuthal Angle θ

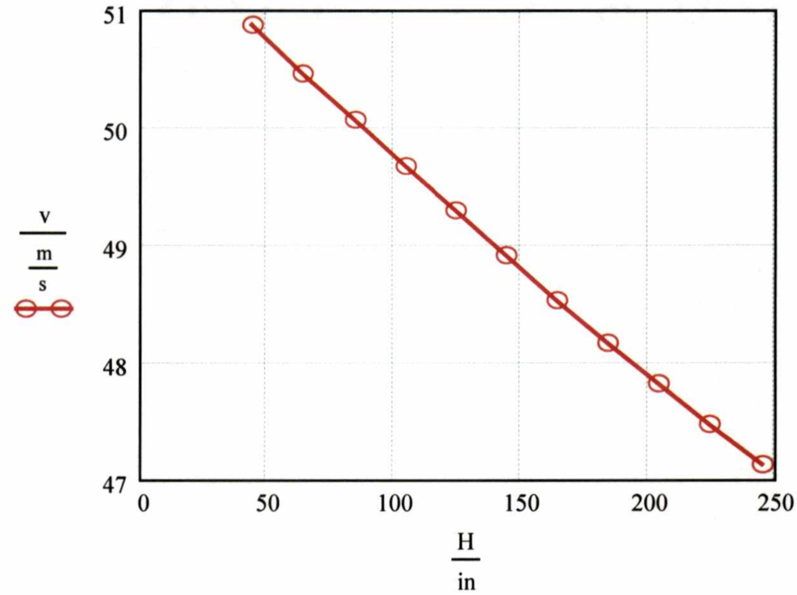

Fig 5.13 The Influence Of Cargo Box Height *H* On Liftoff Speed *v*

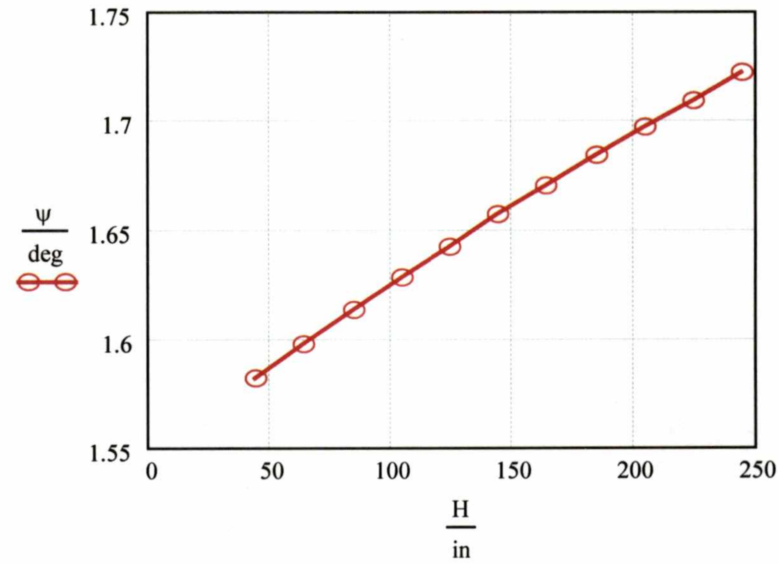

Fig 5.14 The Influence Of Cargo Box Height H On Liftoff Roll Angle ψ

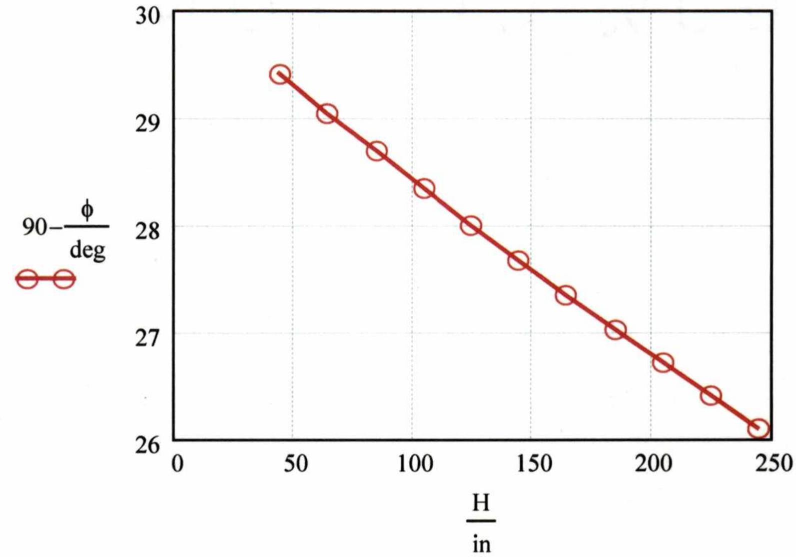

Fig 5.15 The Influence Of Cargo Box Height H On Elevation Angle ϕ

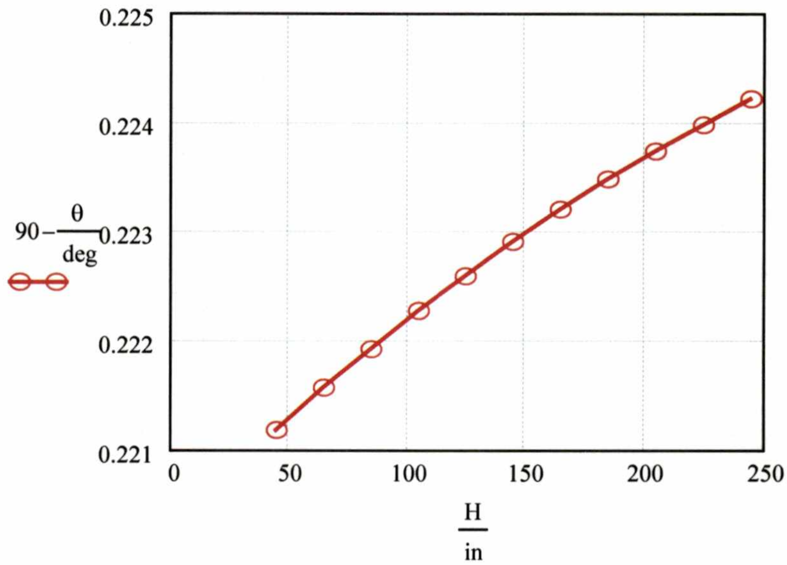

Fig 5.16 The Influence Of Cargo Box Height *H* On Azimuthal Angle θ

5.2.3 The influence of the cargo longitude position *b*

From Fig 5.17 and 5.18 we find when the 500-lbf hung cargo longitudinal position *b* becomes larger, liftoff speed and roll angle both increase, which means liftoff is less likely. When length *b* changes from 143 in to 343 in, liftoff speed increases from 48.78 m/s to 48.93 m/s and roll angle increases from 1.64° to 1.66°. But we find that the improvement is not so significant for either liftoff speed or roll angle with only a 500-lbf cargo.

From Fig 5.19 and Fig 5.20 we can see when the hung cargo moves towards the end of the cargo box, both the lift and the backward movement increase. The elevation angle increases from 27.54° to 27.71° and the azimuthal angle increases from -0.21° to 0.34°. Notice that when the cargo is hung at the front part of the cargo box, the azimuthal angle may even become negative, which means it swings to the forward direction.

5.2.4 The influence of cargo lateral position *f*

From Fig 5.21 and Fig 5.22 we see that when we change the cargo lateral position *t*, we get results that are similar to those discussed in chapter 4. When the hung position moves away from the path center and toward the roll direction, the liftoff speed decreases though the roll angle increases. When it moves towards the path center, the liftoff speed increases but the roll angle decreases. The change for a trailer with a 500-lbf hung cargo is from 48.54 m/s to 49.26 m/s for speed change and from 1.67° to 1.64° for roll angle change. So, the best scheme is to hang the cargo on the centerline of the cargo box.

From Fig 5.23 and Fig 5.24 we can also find the influence of the hanging point offset on the movement of the cargo itself. It lifts from 27.37° to 27.98° when the

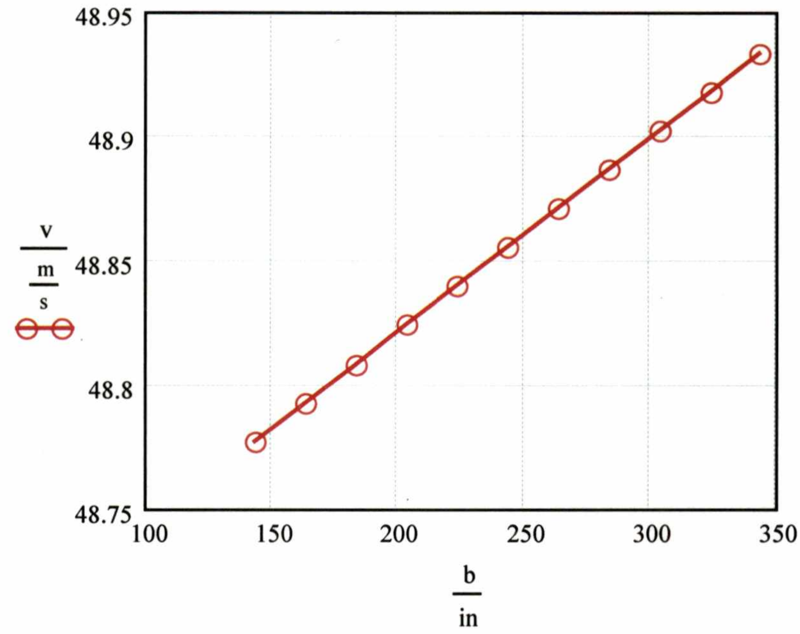

Fig 5.17 The Influence Of Cargo Longitudinal Position *b* On Liftoff Speed *v*

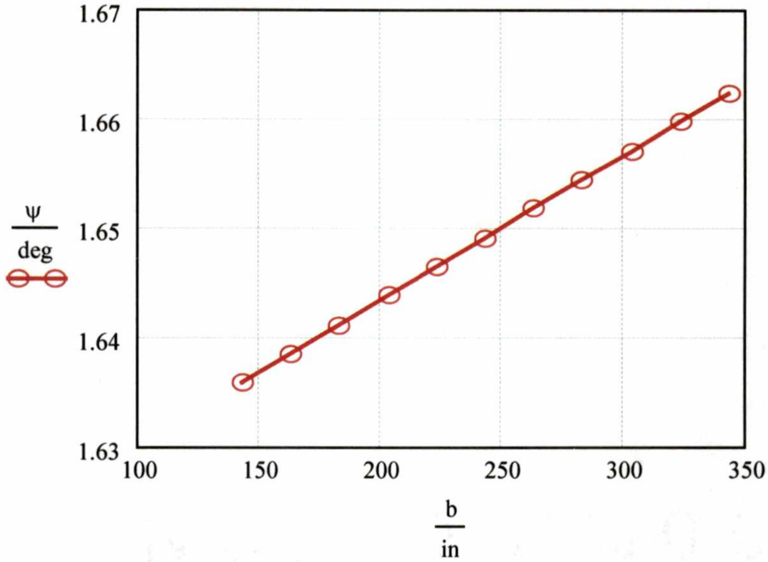

Fig 5.18 The Influence Of Cargo Longitudinal Position *b* On Liftoff Roll Angle ψ

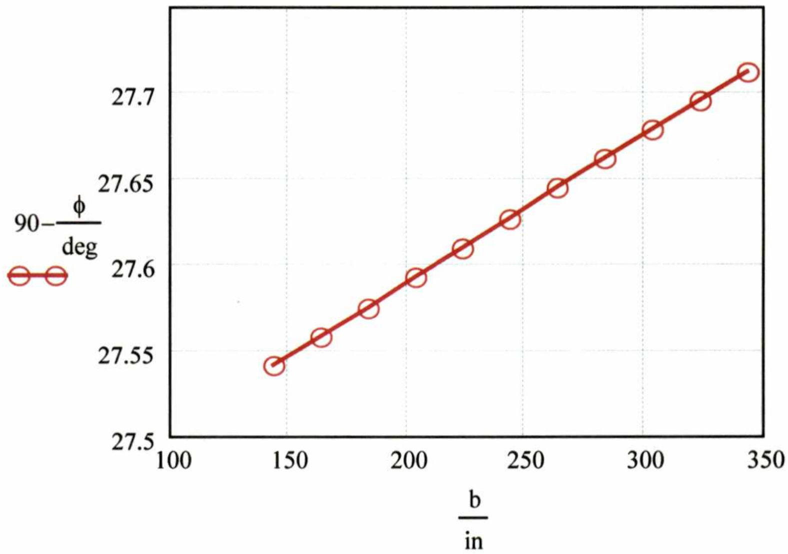

Fig 5.19 The Influence Of Cargo Longitudinal Position *b* On Elevation Angle ϕ

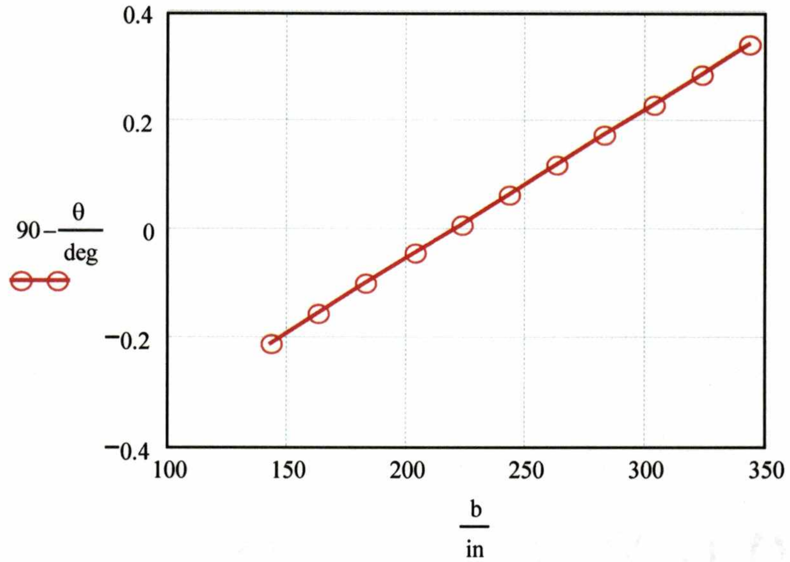

Fig 5.20 The Influence Of Cargo Longitudinal Position *b* On Azimuthal Angle θ

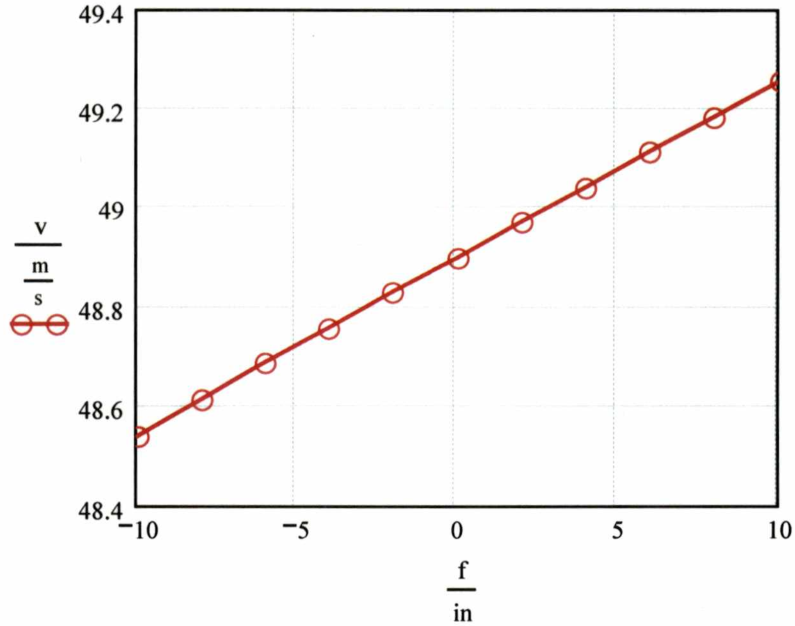

Fig 5.21 The Influence Of Cargo Lateral Position *f* On Liftoff Speed *v*

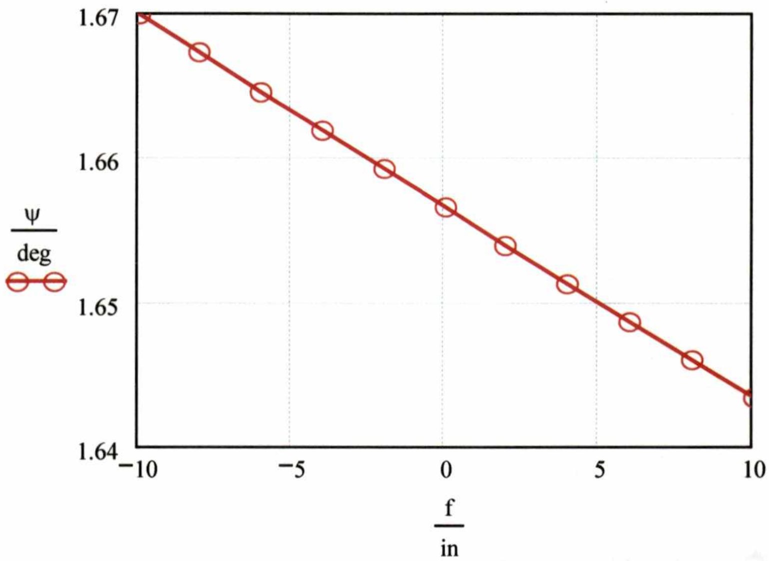

Fig 5.22 The Influence Of Cargo Lateral Position *f* On Liftoff Roll Angle ψ

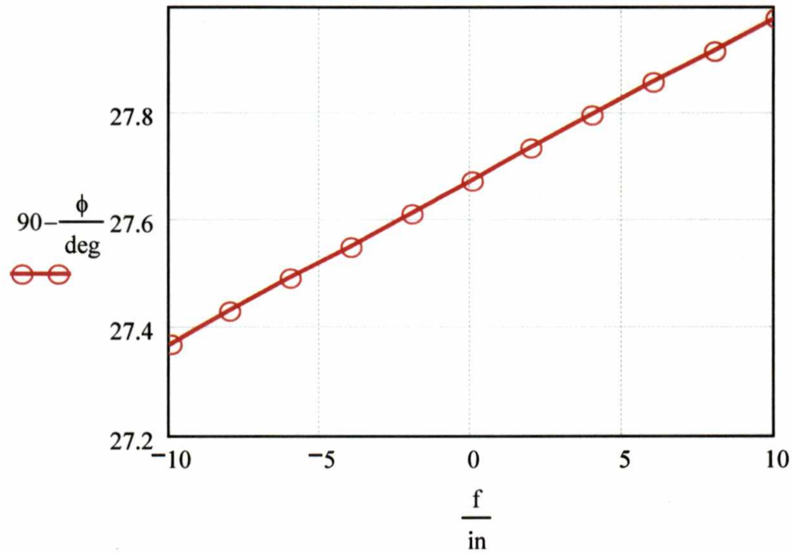

Fig 5.23 The Influence Of Cargo Lateral Position *f* On Elevation Angle ϕ

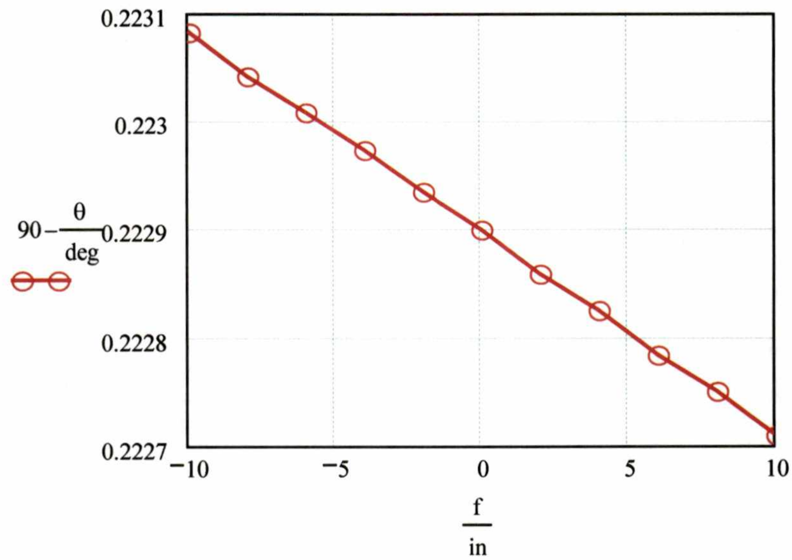

Fig 5.24 The Influence Of Cargo Lateral Position *f* On Azimuthal Angle θ

hanging point moves toward the path center from –10 in to 10 in. The influence on the azimuthal angle is not so significant. It moves forward from 0.2231° to 0.2227° as the hanging position moves 20 in toward path center.

5.2.5 The influence of the length l

Fig 5.25 and Fig 5.26 exhibit the influence of l on the liftoff speed and roll angle of the trailer. We find that liftoff speed decreases slightly from 48.901 m/s to 48.898 m/s as the length increases. However, the liftoff roll angle almost does not change, only changing from 1.6566° to 1.6567°. So, although a longer hung length will reduce roll stability and should be avoided, the influence is very small for a 500-lbf cargo.

Fig 5.27 and Fig 5.28 illustrate the influence of change of length l on the movement of the cargo itself. The elevation angle increases a little bit from 27.67° to 27.68° while l becomes longer. And there is almost no influence on the azimuthal angle at all when l changes.

Though the change of l has some influence on the trailer liftoff properties and cargo movement, it is negligibly small for a 500-lbf cargo.

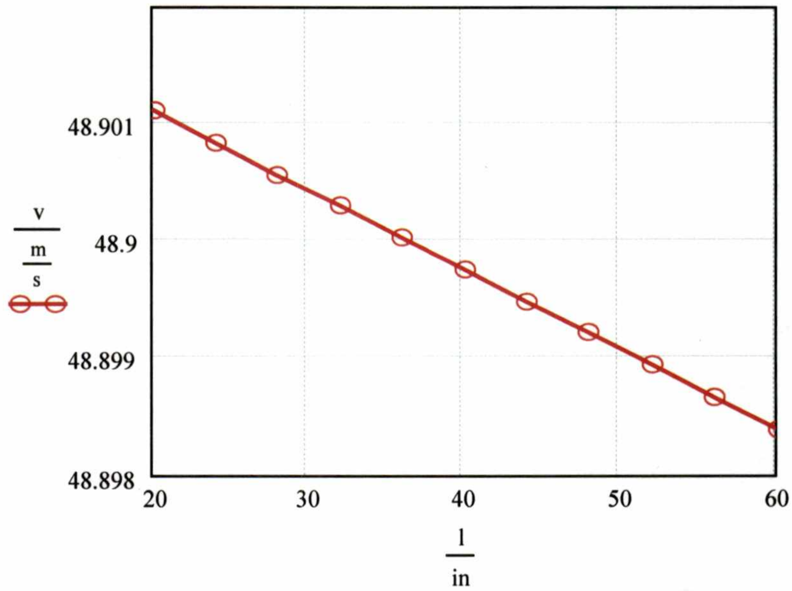

Fig 5.25 The Influence Of Length *l* On Liftoff Speed *v*

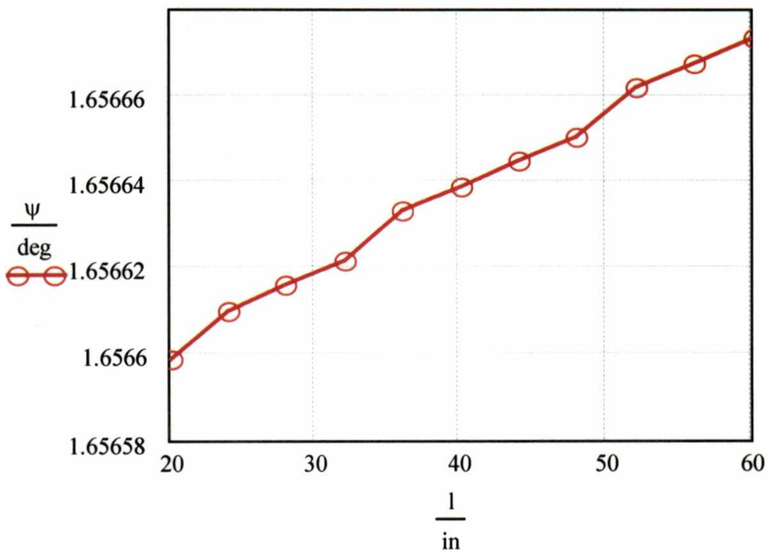

Fig 5.26 The Influence Of Length l On Liftoff Roll Angle ψ

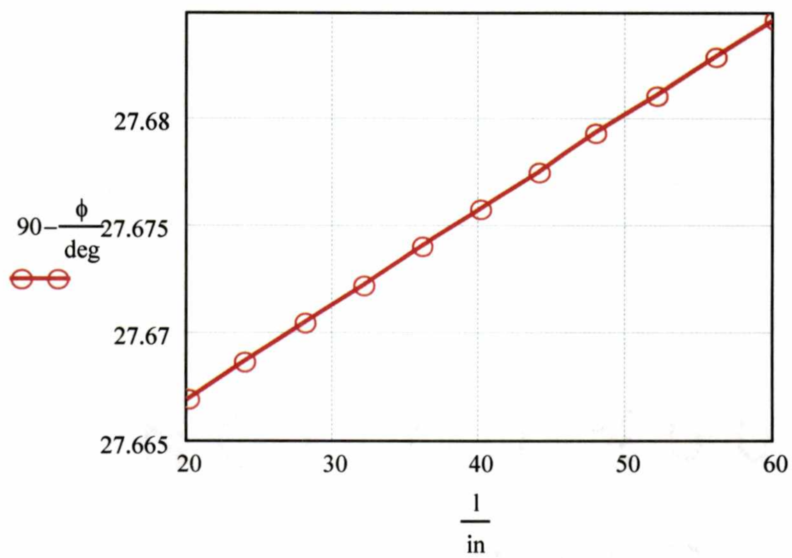

Fig 5.27 The Influence Of Length l On Elevation Angle ϕ

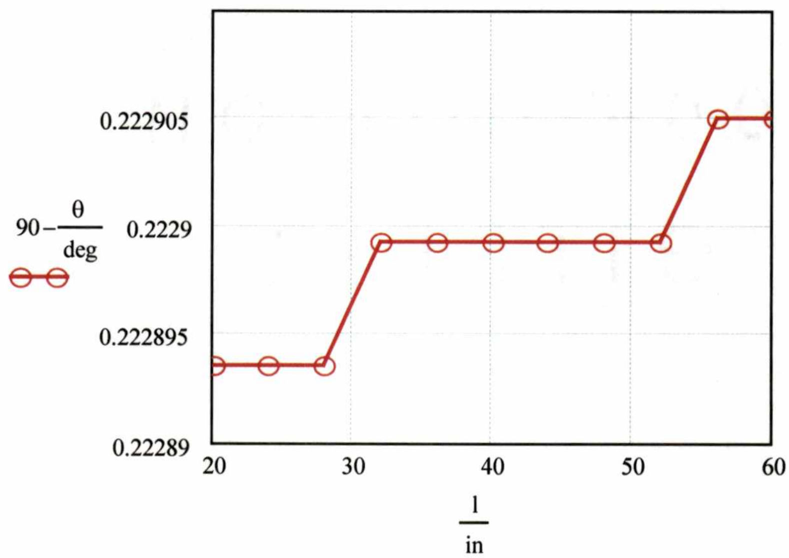

Fig 5.28 The Influence Of Length l On Azimuthal Angle θ

Chapter 6

Conclusions

From the previous discussion we find that the 3-D trailer liftoff model has the following advantages.

- This model predicts the liftoff of the trailer axle instead of the tractor's drive-axle by calculating the roll angle at liftoff and the vehicle speed when this roll angle is attained. Fewer influencing factors are needed to predict trailer axle liftoff than are needed to predict drive-axle liftoff or rollover. If it is eventually validated by experiments with real trucks, the model discussed here should be more convenient than a model that attempts to predict drive-axle liftoff or rollover.
- Since vehicle speed is used as a reference parameter to predict the trailer liftoff, it is easier to get than the lateral acceleration and is easier for the drivers to understand.
- This model does not consider any parameters of the tractor, which makes the model simpler and the calculation faster than for a more complicated model. Because the trailer liftoff properties can be predicted independently of the tractor, even trailer manufacturers could use such a model to gain some information on the liftoff properties of the trailers they produce. This would be especially useful for tank trailers.
- Though the model is very simple, many factors that influence the roll stability of the trailer and cargo can be considered: increasing path radius R, trailer track

width *T*, roll center height *q*, fifth-wheel height *q+d*, trailer suspension roll stiffness *k*, and center of gravity longitudinal distance from the fifth-wheel *a*, and decreasing the center of gravity height *h*, and lateral center of gravity offset *t* can all improve the roll stability and liftoff properties.

- The model has been verified to be consistent with Lagrange's equations.
- The model can be used for a trailer with moving cargo. A simple example is given and many influencing factors are discussed. When there is one hanging cargo in the cargo box, increasing path radius R, longitudinal distance from the fifth-wheel to the hanging point of the cargo b, and decreasing the cargo box height and lateral hanging position f can all improve the liftoff properties and roll stability of the trailer.
- Angular displacement of the hanging cargo can also be obtained through the model.

In general, the three-dimensional rigid body trailer liftoff model is convenient, consistent with Lagrange's equations, and potentially broadly useful.

Chapter 7

Future Research

In the previous chapters, only the simplest motion and loading situation of the trailer are considered. But there are also some other circumstances that one could use this model to solve. There are also some other influencing factors that are not considered in this thesis. If these factors were added, the performance and precision might be improved. There are also steps one could take to validate the accuracy of the model. Finally, the model could serve as the basis for a new rollover warning system.

7.1 Three-Dimensional Trailer Liftoff Model With Multiple Hanging Cargos And Liquid Cargo

After some minor modification, this three-dimensional model can also be used in evaluating the liftoff speed and roll angle when there are many hanging cargos or liquid cargo in the cargo box.

When n cargos are hanging on the ceiling of the cargo box, equation (5.1) becomes

$$(7.1) \qquad \Sigma\overline{M}_A = \overline{r}_{AP}\times\overline{F}_P + \overline{r}_{AC}\times\overline{W}_C - \overline{M}_P + \overline{r}_{AS1}\times\overline{F}_{S1} + \overline{r}_{AS2}\times\overline{F}_{S2} + \ldots + \overline{r}_{ASn}\times\overline{F}_{Sn}\,.$$

Adding with $\Sigma\overline{M}_B$ and taking the dot product of both sides with $\overline{r}_{AB}$ gives

$$(7.2) \qquad \left(\Sigma\overline{M}_A + \Sigma\overline{M}_B\right)\cdot\overline{r}_{AB} = [\overline{r}_{AC}\times\overline{W}_C + \overline{r}_{BQ}\times\overline{W}_U + \sum_{i=1}^{n}\ (\overline{r}_{ASi}\times\overline{F}_{Si})]\cdot\overline{r}_{AB}\,,$$

in which

$$(7.3) \qquad \overline{F}_{Si} = \overline{W}_{Ei} - m_{Ei}\cdot\overline{a}_{Ei}\,.$$

Similarly, there are also

(7.4) $\Sigma \overline{M}_{Ei} = \overline{r}_{SEi} \times \overline{F}_{Si}$, $i = 1,2...n.$

Solving the equation system (5.9), (5.10) and *n* (5.12) can yield the roll angle of the cargo box, the speed at the specified path radius, and the elevation and azimuthal angles of the *n* hanging cargos. (The approach described here would require significant modification if the hanging cargos were allowed to collide with each other or with the cargo box.)

Liquid cargo can also be considered as *n* pieces of continuous cargos "hung" on the floor or on the center of gravity of the cargo box in the longitudinal direction as *n* hanging cargos mentioned above. Similar calculation can be employed to find out the influence of liquid cargo on the liftoff properties.

7.2 Other Factors Needs To Be Considered In The Model

In the previous chapters, only the roll stiffness of the trailer axle is considered in calculating the liftoff properties of the trailer. But there are also some other factors that may affect the precision of the model. Trailer tire properties, trailer suspension and fifth-wheel properties should also be considered to improve the precision of the calculated results.

7.3 Further Validation Of The Model

Validation of the model presented in this thesis has thus far been limited to comparing Newtonian and Lagrangian formulations of the underlying equations of motion. This comparison shows that the mathematics of the model is internally consistent. A broader question is the extent to which the model agrees with reality. As mentioned previously, comparison with experimental results would be the ideal method of answering that question. Lacking such data, one could still learn much about the present model's validity by comparing its predictions with those of more sophisticated software that is known to give results that compare favorably with experimental results. Details of such a comparison are under development.

References

References

J.A.M. Boulet, *Trailer Dynamics*. November 29, 1999. Personal communication.

National Automotive Sampling system (NASS) General Estimates System (GES) Analytical User's Manual 1998-1997. Washington, DC: U.S. Department of Transportation; National Highway Traffic Safety Administration; National Center for Statistics and Analysis, June 1998.

Truck and bus accident fact book, 1995. Special report. Michigan University, Ann Arbor, Transportation Research Institute.

Jerry H. Ginsberg, Georgia Institute of Technology,1995, *Advanced Engineering Dynamics*, Second Edition, Cambridge University Press.

Mathcad User's Guide with Reference Manual 2001, Math Soft Company.

L. Segel and R. D. Ervin, 1981, "*The Influence of Tire Factors on Trucks and Tractor-Trailers.*" Vehicle System Dynamics, Vol. 10, No. 1, February 1981.

C. Mallikarjunarao, and L. Segel, 1981, "*A study of the directional and roll dynamics of multiple articulated vehicles*", Proceedings of the 7th IAVSD Symposium on the Dynamics of Vehicle Roads and Trucks, Cambridge, England.

C. Mallikarjunarao, R. D. Ervin and L. Segel, 1982, " *Roll Response of Articulated Motor Trucks During Steady-Turning Maneuvers.*" Presented at the ASME Annual Winter Meeting, Phoenix, Ariz., November 14-19, 1982.

C. C. MacAdam, 1982, "*A Computer-Based Study of the Yaw/Roll Stability of Heavy Trucks Characterized by High Centers of Gravity.*" SAE paper No. 821260.

R. D. Ervin, 1983, "*The Influence of Size and Weight Variables on the Roll Stability of Heavy Duty Trucks.*" SAE paper No. 831163.

R. D. Ervin, 1986, "*The Dependence of Truck Roll Stability on Size and Weight Variables.*" Int. J. of Vehicle Design, Special Issue on Vehicle Safety, pp192-208, 1986.

R. D. Ervin, C. C, MacAdam, M. A. Barnes, 1987, "*Truck Control Problems Posed by the Design of Highway Ramps*" SAE paper No. 870071.

D. D. Furleigh, M. J. Vanderploeg and C. Y. Oh, 1988, "*Multiple Steered Axles for Reducing the Rollover Risks of Heavy articulated Trucks.*" SAE paper No. 881966

L. A. Laird, 1988, "*Measurement of Heavy Vehicle Suspension Roll-Stability Properties, and a Method to Evaluate Overall Stability Performance.*" SAE paper No. 881869

Shinsuke Miki, 1988, "*Method for Evaluating Stability and Handling of a Truck Considering Body Torsional Rigidity.*" SAE paper No. 881870.

J. Bernard, J. Shannan and M. Vanderploeg, 1989, "*Vehicle Rollover on Smooth Surfaces*", SAE paper No. 891991.

S. Rakheja and A. Piche, 1990, "*Development of Directional Stability Criteria for an Early Warning Safety Device*", SAE paper No. 902265.

C. B. Winkler, S. M. Karamihas, and S. E. Bogard, 1992, "*Roll Stability Performance of Heavy Vehicle Suspension*", SAE paper No. 922426.

F. P. D. Navin, 1992, "*Estimating Truck's Critical Cornering Speed and Factor of Safety*", J. of Transportation Engineering, Vol. 118, No. 1, January/February, 1992.

M. El-Gindy, 1992, "*The Use of Heavy Vehicle Performance Measures for Design and Reglation*", Transportation Systems, Vol 44, pp367-382, 1992.

N. S. Das, B. A. Suresh, and J. C. Wambold, 1993, "*Estimation of Dynamic Rollover Threshold of Commercial Vehicles Using Low Speed Experimental Data*", SAE paper No. 932949.

M. El-Gindy, L. Tong and B. Tabarrok, 1993, "*Frequency Response Analysis of Canadian Logging Trucks.*" Vehicle System Dynamics, Vol. 23, No. 5, July 1994. pp325-349, 1994.

R. C. Lin, D. Cebon, and C. J. Cole, 1996, "*Active Roll Control of Articulated Vehicles*", Vehicle System Dynamics, Vol. 26, No. 1, July 1996. pp17-43, 1996.

P. J. Liu, S. Rakheja, and A. K. W. Ahmed, 1997, " *Detection of Dynamic Roll Instability of Heavy Vehicles for Open Loop Rollover Control*", SAE paper No. 973263.

S. McFarlane, P. Sweatman, P. Dovile, and J. Woodrooffe, 1997, " *The Correlation of Heavy Vehicle Performance Measures*", SAE paper No. 973190.

E. Dahlberg, N. G. Vagstedt, 1997, " *The Advantages of a Simple Approach Modeling Heavy Vehicle Handling*", SAE paper No. 973264.

P. J. Liu, S. Rakheja and A. K. W. Ahmed, 1998, "*Dynamic Rollover Threshold of Articulated Freight Vehicles*", Heavy Vehicle Systems, Int. J. of Vehicle Design, Vol. 5, Nos3/4, 1998, pp 300-322.

C. B. Winkler, D. Blower, R. D. Ervin, 1999, "*Rollover of Heavy Commercial Vehicles*", University of Michigan, Transportation Research Institute, 61p, sponsor: Volvo truck Corporation, AB, Great Lakes Center for Truck and Transit Research. UMTRI-99-19, Revised Edition.

Appendix

Data Used in the Model*

Name of Data	Symbol	Units	Dimension	Range if changed
distance from fifth wheel center to trailer roll center	L	ft	40.5	
longitude center of gravity position of empty cargo box	a	in	300	143~343
trailer axle track width	T	in	72	62~82
lateral position of cargo box center of gravity	t	in	0	-10~10
height of fifth-wheel over roll center	d	in	20	10~30
height of roll center over undercarriage center of gravity	p	in	9.5	
cargo box center of gravity height over fifth-wheel	h	in	22	12~32
roll center height	q	in	29	19~39
trailer axle roll stiffness	k_0	in.lbf/deg	140,000	90,000~190,000
empty cargo box weight	W_C	lbf	10,800	
undercarriage weight	W_Q	lbf	3,000	
empty cargo box roll moment of inertia	I_{C11}	in.lb.sec^2	80,000	
empty sprung mass pitch and yaw moment of inertia	I_{C22}, I_{C33}	in.lb.sec^2	1,328,867	
undercarriage mass roll moment of inertia	I_{Q11}	in.lb.sec^2	8,100	
undercarriage mass pitch moment of inertia	I_{Q22}	in.lb.sec2	6,735	
undercarriage mass yaw moment of inertia	I_{Q33}	in.lb.sec^2	11,066	
loaded cargo box weight	W_C	lbf	57,500	
longitude center of gravity position for loaded cargo box	a	in	301.56	
loaded cargo box roll moment of inertia	I_{C11}	in.lb.sec^2	307,910	
loaded cargo box pitch and yaw moment of inertia	I_{C22}, I_{C33}	in.lb.sec^2	4,842,462	
hung cargo longitude position from fifth-wheel	b	in	300	143~343
hung cargo lateral position	f	in	0	-10~10
length from cargo hung point to hung cargo center of gravity	l	in	40	20~60
height of cargo box	H	in	144	44~244
hung cargo weight	W_E	lbf	500	100~1000

*(Fancher, Ervin, Winkler, Giliespie, 1986)

Vita

Junyu Li was born in Zhangjiakou, Hebei Province, P. R. China on April 3rd, 1970. She spent her childhood in Shenyang, Liaoning province and moved to Changchun, Jilin province in 1980. There in Changchun, she attended the City Experimental High School and graduated in 1988. She then joined Jilin University of Technology and got her Bachelor and Master's Degree in Engineering in 1992 and 1995 respectively. Since April 1995, she had been working in Changchun Automotive Research Institute of the First Automotive Works of China as a car development and design engineer.

Since August 1999, she has been enrolled in the graduate program in the Mechanical and Aerospace Engineering and Engineering Science Department at the University of Tennessee, Knoxville. Her research area here is automotive dynamics. Upon successful defense of the thesis, Junyu Li will receive her Master of Science in Engineering degree.